

Assessing the effects of restoration and conservation on gaseous carbon fluxes and climate mitigation capacity across six European coastal wetlands

Miguel Cabrera-Brufau^{*a}, Camille Minaudo^a, Katrin Attermeyer^b, Alba Camacho-Santamans^a, Rafael Carballeira^c, Benjamin Misteli^b, Jorge Montes-Pérez^a, Daniel Morant^c, Biel Obrador^a, Antonio Picazo^c, Carlos Rochera^c, Mihai Adamescu^d, Raquel Ambrosio^e, Giancarlo Bachi^f, Nina Bègue^e, Martynas Bučas^g, Lúdia Cañas Ramírez^a, Marco Carloni^f, Lamara Cavalcante^h, Constantin Cazacu^d, Giovanni Checcucci^f, J. Pedro Coelho^h, Valentin Dinu^d, Valtere Evangelista^f, Ilenia Férez Martín^a, Jonas Gintauskas^g, Relu Giuca^d, Anis Guelmami^e, Mirco Guerrazzi^f, Samuel Hilaire^e, Marija Kataržytė^g, Ana I. Lillebø^h, Raquel Lizán^c, Bruna R.F. Oliveira^h, Vitor H. Oliveira^h, Marta Pedrón^c, Jolita Petkuvienė^g, Tudor Racoviceanu^d, Michael Ronse^e, Chiara Santinelli^f, Ana I. Sousa^h, Wouter Suykerbuykⁱ, Edvinas Tiškus^g, Claudia Tropea^f, Diana Vaičiūtė^g, Silvia Valsecchi^f, Marinka van Puijenbroekⁱ, Mourine J. Yegon^b, Antonio Camacho^{ct}, Daniel von Schiller^{at}

^aDepartament de Biologia Evolutiva, Ecologia i Ciències Ambientals, Universitat de Barcelona, Av. Diagonal 643, 8028, Barcelona, Spain

^bWasserCluster Lunz - Biologische Station, University of Vienna, Dr. Carl Kupelwieser Promenade 5, 3293, Lunz am See, Austria

^cInstitut Cavanilles de Biodiversitat i Biologia Evolutiva, Universitat de València, C/Catedratic José Beltrán 2, 46980, Paterna, Spain

^dDepartment of Systems Ecology and Sustainability, University of Bucharest, spl. Independentei 91 - 95, 50095, Bucharest, Romania

^eInstitut de recherche pour la conservation des zones humides méditerranéennes, Tour du Valat, Le Sambuc, 13200, Arles, France

^fIstituto di Biofisica, Consiglio Nazionale delle Ricerche (CNR) Pisa, Via Giuseppe Moruzzi 1, 56124, Pisa, Italy

^gMarine Research Institute, Klaipėda University, Universiteto ave. 17, 92294, Klaipėda, Lithuania

^hECOMARE, CESAM - Centre for Environmental and Marine Studies, Department of Biology, University of Aveiro, Campus de Santiago, 3810-193, Aveiro, Portugal

ⁱWageningen Marine Research, Wageningen University & Research, Korringaweg 7, 4401 NT, Yerseke, The Netherlands

[†]These authors share last authorship as research heads

^{*}Corresponding author, email: miguelcabrera@ub.edu

This manuscript is a non-peer reviewed preprint submitted to [EarthArXiv](https://www.eartharxiv.org/). It was submitted to the [Journal of Environmental Management](https://www.journals.elsevier.com/journal-of-environmental-management/) for peer review on 23/12/2025.

Abstract

Coastal wetlands play a substantial role in regulating Earth's climate through exchanges of greenhouse gases (GHGs). Current European policies promote widespread coastal wetland restoration to reverse historical losses and ongoing pressures. However, substantial uncertainty remains regarding how CO₂ and CH₄ fluxes respond to restoration across different coastal wetland types and whether these responses translate into net climate mitigation in terms of CO₂ equivalents (CO₂-eq). We measured simultaneous CO₂ and CH₄ fluxes using static chambers across four seasons at multiple locations spanning preserved, altered and restored sites within each of six European coastal wetlands of different ecological types. By comparing GHG exchanges and resulting CO₂-eq balances across wetlands, we identified the dominant biogeochemical drivers of CO₂ and CH₄ dynamics and assessed the climate mitigation potential of conservation and restoration actions. CO₂ fluxes were primarily controlled by landscape-scale vegetation cover and inundation, whereas CH₄ emissions responded to more subtle changes in water quality, salinity and wetland hydrodynamics. Comparisons of CO₂-eq balances between altered and restored sites revealed that seagrass replantation and eutrophication reversal generated significant mitigation benefits, driven by enhanced CO₂ uptake and reduced CH₄ emissions, respectively. In contrast, other restoration measures modified CO₂ and CH₄ fluxes in opposing directions, resulting in non-significant net climatic effects of CO₂-eq balances. Overall, our results demonstrate that climate mitigation outcomes of coastal wetland restoration are both GHG-specific and wetland-type dependent, underscoring the need for tailored restoration strategies and robust, multi-GHG monitoring to detect and accurately quantify potential climatic benefits.

Keywords: coastal wetlands, ecological restoration, CO₂ fluxes, CH₄ fluxes, climate change mitigation

1. Introduction

Coastal wetlands are relevant components of the global carbon (C) cycle and are widely recognized as blue carbon ecosystems. Despite their relatively low areal extent, they exert a disproportionate influence on the global climate by providing long-term C-sequestration and regulating atmospheric greenhouse gas (GHG) concentrations (Mitsch et al., 2012). Wetlands in good conservation status are highly productive ecosystems, where low oxygen availability limits aerobic organic matter degradation, resulting in net uptake of carbon dioxide (CO₂) and sequestration of C in sediments and biomass (Reddy et al., 2022). At the same time, wetland anoxic sediments act as hot spots for methane (CH₄) emissions, making up 20-30% of global CH₄ emissions (Saunio et al., 2016), particularly when they are degraded by alterations enriching the organic content such as eutrophication (Morant et al., 2020a, 2020b). While the magnitude of CO₂ exchanges typically exceeds that of CH₄, the higher global warming potential of the latter has the potential to overcome the effects of CO₂ uptake and might result in a net balance that favors atmospheric warming (Canadell and Monteiro, 2023). Ultimately, the net radiative forcing of coastal wetlands is largely determined by the net balance of CO₂ and CH₄ exchanges with the atmosphere.

Diverse historical and current pressures have led to important reductions of the extent and quality of global wetland ecosystems (Fluet-Chouinard et al., 2023). While areal loss quantification remains challenging, especially when assessing coastal zones with high historical development and land-reclamation practices, estimates of European coastal wetland loss exceed 65% during the last century (Airoldi and Beck, 2007). Further, the majority of remaining European wetlands have a poor or bad ecological status (European Environment Agency, 2024) and experience diverse natural and anthropogenic pressures (Maes et al., 2020). Although conservation policies, such as those under Ramsar (Ramsar Convention, 1971) and the UE habitats Directive, help preserve the remaining wetlands, their historical losses mean that widespread restoration is still needed. In this context, the recent EU Nature Restoration Regulation aims at reverting this widespread degradation and recovering crucial ecosystems services lost (European Union, 2024). Among the potential benefits of restoration, climate change mitigation is increasingly being used as a supporting argument. However, large uncertainties remain on the climatic mitigation capacity of coastal wetland restoration (Jones et al., 2024).

Coastal wetlands influence climate primarily through CO₂ and CH₄ exchange, governed by the balance among photosynthesis, aerobic and anaerobic respirations releasing CO₂, as well as methanogenesis (Reddy et al., 2022). While local climate and wetland type shape baseline GHG fluxes (Camacho et al., 2017), ecosystem alteration and restoration can modify these fluxes by changing key controls, including vegetation, nutrient inputs, hydrology, salinity, and sediment redox conditions (Camacho-Santamans et al., 2025; Morant et al., 2024). The biomass and type of dominant primary producers exert a large impact on the primary productivity of wetlands, as they represent the basic functional standing stock for photosynthetic CO₂ uptake. While nutrients are essential to maintain plant photosynthetic rates, excessive nutrient loads, namely nitrogen and phosphorus, can lead to eutrophication and uncontrolled proliferation of benthic algae and phytoplankton blooms (Zilius et al., 2013). This shift in primary producers results in a cascade of biogeochemical consequences, including anoxia and organic matter degradation through methanogenesis, that ultimately lead to severely enhanced CH₄ emissions (Bonaglia et al., 2025). Wetland hydrology is one of the key factors regulating ecosystem functioning, as it

influences both primary production through water availability and the balance between respiration and methanogenic degradation of organic matter through limitation of oxygen diffusion into the sediments (Cui et al., 2024; Rochera et al., 2025a). However, anoxic conditions do not always result in elevated wetland CH₄ emissions, as the supply of sulfate by saline waters can severely limit methanogenesis through resource competition with more energy-efficient sulfate reduction metabolisms under the right redox conditions (Lovley and Klug, 1983; Miralles-Lorenzo et al., 2025). Emissions of CH₄ are further modulated by the existence of plant-mediated transport mechanisms, which can bypass oxidation back to CO₂ during upward diffusion through oxic sediment horizons (Ge et al., 2024).

While the general biogeochemical controls of wetland CO₂ and CH₄ exchanges are relatively well understood, large uncertainty remains on how these interact under practical cases of ecological restoration, leading to poorly constrained climatic mitigation potential (Griscom et al., 2017). Wetland restoration generally enhances CO₂ uptake outweighing increases in CH₄ emissions and resulting in net climate benefits (He et al., 2024). However, existing literature is dominated by studies focused on inland systems (peatlands) and just a few coastal wetland types (mangroves, saltmarshes), which do not capture coastal wetland diversity accurately (Misteli et al., 2025; Taillardat et al., 2020). Other synthesis efforts on coastal wetland restoration focus exceedingly on C sequestration (i.e., *Blue Carbon*), overlooking the large role of CH₄ emissions on the net climatic outcome of wetland restoration (Bertolini and da Mosto, 2021). In addition, while valuable for identifying broad patterns, global syntheses often aggregate the high diversity of wetland types, alteration histories and restoration strategies into a limited number of categories (O'Connor et al., 2020), thereby obscuring relevant contextual factors and limiting process-based effective transferable knowledge for management. Overall, current evidence is still scarce on how coastal wetland restoration influences GHG fluxes (Macreadie et al., 2019; Misteli et al., 2025) and coordinated, multi-site assessments are needed to reveal common controls that are robust across wetland types and restoration pathways.

In order to better understand the climate mitigation potential of restoring and conserving European coastal wetlands, this study examines concomitant CO₂ and CH₄ exchanges and their combined carbon dioxide equivalent (CO₂-eq) climatic effect across six diverse European case pilot coastal wetlands: saltmarshes, seagrass meadows, freshwater and brackish marshes, riverine lakes and freshwater coastal lagoons. By explicitly embracing the diversity of coastal wetland types, conservation status, and restoration pathways represented across Europe, we aim to move beyond site-specific assessments and identify common patterns and drivers governing GHG flux responses to alteration and restoration. Using standardized static chamber measurements conducted during four seasonal sampling campaigns, we compare instantaneous GHG exchanges across wetland sites representative of preserved, altered, and restored status. Our objectives are to (i) systematically identify the main biogeochemical drivers controlling CO₂ and CH₄ fluxes in the main European coastal wetland types, and (ii) quantify the extent to which restoration and conservation modify their net climatic effect, expressed as daily CO₂-eq fluxes. We hypothesize that (i) the drivers and sensitivity of GHG fluxes to the conservation status differ between CO₂ and CH₄, reflecting their distinct production and consumption pathways, and that (ii) the net climatic response to restoration depends on both the type of anthropogenic alteration and the wetland type considered. At the same time, we expect that consistent

cross-system patterns will emerge, allowing the identification of shared controls on GHG fluxes despite the heterogeneity of wetland types and restoration contexts examined.

2. Methods

2.1. Study areas

Six case pilots were strategically selected to cover a wide range of European coastal wetland types, thereby providing a representative sample of the ecosystem and climatic diversity across the continent, covering major European coastlines (Atlantic, Mediterranean, Black Sea, Baltic Sea). The selected case pilots were (**Figure 1, Figure S1**): South-West Dutch Delta (DU, intertidal salt marshes, Netherlands), Ria de Aveiro (RI, intertidal seagrass beds, Portugal), Camargue (CA, freshwater marshes and ponds, France), the Valencian wetland Marjal dels Moros (VA, brackish marshes, Spain), Danube Delta (DA, freshwater lakes and ponds with reed beds, Romania) and Curonian Lagoon (CU, freshwater lagoon with reed and submerged vegetation, Lithuania). Within each case pilot, sites representing three conservation statuses were selected in duplicate: preserved, altered, and restored. Preserved sites served as reference systems with unaltered structure and function, whereas altered and restored sites reflected dominant anthropogenic pressures and corresponding restoration measures. Sites within each pilot wetland were geographically close, ensuring comparable climatic conditions and allowing differences in biogeochemical functioning to be attributed to the conservation status. Site characteristics are summarized in **Table 1**, with further details provided in supplementary materials and Oliveira et al. (submitted).



Figure 1. Map showing the location of the six case pilots. Map lines do not necessarily depict accepted national boundaries. Representative pictures can be found in **Figure S1**.

Table 1. Summary descriptions of studied wetland type, main alterations and restoration activities for each of the six case pilots.

Case pilot	Wetland type	Alteration	Restoration
South-West Dutch Delta (DU)	Intertidal salt marshes	Erosion-protection coastal infrastructures	Removal of barriers and passive saltmarsh recovery
Ria de Aveiro (RI)	Intertidal <i>Zostera noltii</i> seagrass meadows	Bait-digging, trampling, vegetation loss	Active re-vegetation (transplantation)
Camargue (CA)	Freshwater marshes and ponds	Land-use change and artificial hydrological regime	Habitat reconstruction (Soil, hydrology, morphology, vegetation)
Marjal dels Moros (VA)	Brackish marshes	Desalination, hydromorphological and soil degradation, invasive species	Habitat reconstruction (Soil, hydrology, morphology, vegetation)
Danube Delta (DA)	Freshwater lakes and ponds with reed beds	Land-use change (crops and livestock)	Habitat reconstruction (hydrology, morphology, vegetation)
Curonian Lagoon (CU)	Freshwater littoral with submerged vegetation and reed beds	Water quality (eutrophication)	Passive restoration through the reduction of nutrient load and hydrological changes.

2.2. Sampling design

A standardized sampling protocol using static chamber GHG flux measurements was applied across all case pilot wetlands (Minaudo et al., 2023). All 36 sites were sampled once per season, between October 2023 and August 2024. In each site, the areal proportion of three land cover strata classes was estimated in advance using aerial photography and remote sensing images, then confirmed visually upon arrival: (i) open water areas (i.e., without emergent vegetation and with >10 cm of water depth), (ii) vegetated areas (i.e., covered by emergent vegetation (helophytes, and, for Ria de Aveiro, seagrasses), regardless of water presence), and (iii) bare areas (i.e., covered by soil or sediment exposed to the atmosphere at the sampling time). Strata representing <10% of the site area at the time of the visit were excluded from sampling. Each remaining stratum was sampled with a minimum of 3 static chamber deployments, with additional deployments allocated proportionally to stratum areal cover and randomly distributed within each of them. On each sampling day, an average of 15 ± 2 (mean \pm SD) chamber deployments per site were performed, depending on logistical constraints.

All chamber deployments included a dark incubation to minimize heating effects (Lorke et al., 2015). In vegetated areas, an additional transparent incubation was performed to assess the effects of photosynthesis on GHG fluxes. Concentrations of CO₂, CH₄, and H₂O were measured by recirculating chamber headspace through portable gas analyzers (Licor 7810, Picarro G4301, GLA132-GGA). Incubation start and end times were recorded manually and, whenever possible, via instrument software. Two different custom-built static chambers were used depending on the strata. Open water fluxes were measured using a floating opaque semi-spherical chamber ($V = 14.4$ L, $A = 1134$ cm², **Figure S2**) with 10-15 min incubations to capture diffusive and ebullitive fluxes. Bare and vegetated areas were sampled using a modular transparent cylindrical plexiglass chamber with 3-5 min

incubations; collars were inserted 1-3 cm into the sediment and dark conditions were ensured by covering the chamber with an opaque blanket. Chamber volume ($V = 4.6$ to 69 L, $A = 460$ cm², **Figure S2**), was adjusted to vegetation height to optimize sensitivity. In flooded vegetated areas, and to avoid mobilization of sediment CH₄, the chamber was maintained on the water surface either using a flotation ring (**Figure S2**) or holding it by hand. Effective chamber volume was calculated for each deployment based on chamber height above the water and sediment surface.

2.3. Flux calculation

2.3.1. Instantaneous flux estimates

All data treatment, including flux calculations and statistical analyses, was performed in R version 4.5.0 (R Core Team, 2025). Incubation time periods were mapped onto the raw gas concentration time series and start-end times adjusted to exclude instrument and manipulation artefacts after individual visual inspection of each incubation. Ebullitive patterns of CH₄ timeseries were identified but not excluded. A total of 52 CO₂ (1.7%) and 56 CH₄ (1.8%) time series were discarded due to severe artifacts or documented manipulation errors. For the remaining 2,990 CO₂ and 2,986 CH₄ time series, instantaneous fluxes were estimated independently for each gas species using three approaches: (i) a two-point method, where the flux was calculated from the net concentration change throughout the incubation using the average (10 s) initial and final concentrations; (ii) a linear model (LM); and (iii) a non-linear (HM) (Hutchinson and Mosier, 1981) regression model. LM and HM models were obtained using the goFlux R package v2.0.0 (Rheault et al., 2024). Areal molar fluxes were calculated for each of the three approaches via the ideal gas law using chamber geometry, and site-specific temperature and atmospheric pressure recorded by the nearest meteorological station. For each gas time series, a best-flux estimate was selected from the three available models following sequential objective criteria (see supplementary materials). The resulting dataset, containing 2,990 CO₂ and 2,986 CH₄ instantaneous fluxes from 2,106 static chamber deployments, is deposited at LifeWatch ERIC (Cabrera-Brufau et al., 2025).

2.3.2. Data filtering and pooling of non-vegetated strata

To ensure comparability across case pilots and conservation statuses, deployments conducted outside site boundaries or after substantial manipulation (e.g., vegetation removal) were discarded (54 deployments). In the two tidally influenced case pilots (Ria de Aveiro and Dutch delta), deployments during rising and receding tides were also discarded (93 deployments), due to the transient nature of peak-fluxes under these conditions (Lin et al., 2024) and the difficulty of attributing them to the conservation status of the location where they were obtained. Therefore, all subsequent analyses for these case pilots refer only to low-tide conditions. Overall, 147 of the 2,106 deployments with valid fluxes (7%) were excluded from further analysis. Additionally, to ensure strata representativity across statuses and seasons within each case pilot, the three sampled strata were pooled into two classes based on the presence or absence of emergent vegetation (vegetated vs. non-vegetated), enabling robust assessment of strata-specific status effects.

2.3.3. Daily temporal integration and calculation of CO₂ equivalent flux

Instantaneous fluxes were temporarily integrated into a single net daily flux for each chamber deployment, accounting for stratum-specific incubation availability. For

vegetated strata, net daily fluxes were calculated by scaling transparent and dark instantaneous fluxes to the respective daytime and nighttime fractions at each site and date, based on official sunrise and sunset times calculated with the `suncalc` R package (Thieurmél and Elmarhraoui, 2022). For non-vegetated strata, net daily fluxes were derived either directly from a single dark instantaneous measurement (1,087 chambers, 94.7%) or, when both dark and transparent incubations were available due to visible microphytobenthos (61 chambers, 5.3%), using the same temporal scaling approach applied to vegetated strata. Daily combined climatic effect as CO₂-eq flux was calculated for each chamber deployment using the daily CO₂ and CH₄ fluxes and a 100-year global warming potential factor of 27 for CH₄ mass flux (IPCC, 2023). In total, 1,917 CO₂, 1,916 CH₄, and 1,887 CO₂-eq daily fluxes were obtained. Fluxes are reported as daily molar CO₂ and CH₄ fluxes per unit area and time, or as daily CO₂-eq mass fluxes per unit area and time (Neubauer, 2021).

2.4. Statistical treatment

To assess the effects of the conservation status on GHG fluxes, generalized linear mixed effects models (GLMM) were built for each case pilot and net daily flux type (CO₂, CH₄, CO₂-eq). Data was transformed using the `bestNormalize` package (Peterson, 2021). A pseudo-log transformation from the `scales` package (Wickham et al., 2025), a variant of a signed-log transformation that transitions to linear scale at low values near zero, was added to the default `bestNormalize` function options, and the transformation that maximized normality was used for each model. Daily flux was modelled as a function of status, season, vegetation presence, and their full interaction as fixed effects. Site was included as random effect to account for repeated samplings across seasons and for site-specific intercepts. Gaussian-distribution models were preferentially used; T-family distribution models were used when gaussian assumptions were not met. For Ria de Aveiro, vegetation presence was not included as fixed effect due to the absence of non-vegetated areas in restored sites. Models were built using the `glmmTMB` package (McGillucuddy et al., 2025) and validated using DAHRMa diagnostics (Hartig, 2024).

Estimated marginal means (EMMs) were derived for relevant fixed effects using the `emmeans` package (Lenth, 2025). EMMs were weighted by the seasonal areal proportions of vegetated and non-vegetated cover, while maintaining equal seasonal weighting overall; for Ria de Aveiro, equal weights were applied across seasons. Standard errors and confidence intervals accounted for the full variance-covariance structure of each model.

To compare fluxes among conservation statuses and estimate restoration and conservation mitigation capacity, post-hoc pairwise contrasts between EMMs were performed using t or z tests (for gaussian or t-family models, respectively) following the `emmeans` package approach (Lenth, 2025). For each comparison, the difference in EMMs was divided by the standard error of the difference (computed as the square root of the sum of squared standard errors), and two-sided p-values were obtained from the appropriate distribution (normal or t distribution). To account for multiple comparisons within each grouping, p-values were adjusted using the Sidak correction. Letters (Compact Letter Display, CLD) were assigned to significantly different EMMs groups in figures using the `multcompView` package (Graves et al., 2024). All model-derived estimates (EMMs and contrasts) were back-transformed to original scales. Figures were produced with `ggplot2` package (Wickham, 2016). A 5% significance threshold was set for all statistical tests.

Scripts used for statistical treatment of data and figures can be found in https://github.com/MCabreraBrufau/CabreraBrufau_et_al_2026_code.

2.5. Methodological considerations

Several limitations affect the representativity of the GHG flux estimates. Static chamber measurements are prone to closing/opening artefacts and non-linear patterns (Maier et al., 2022). These were mitigated through careful handling, timeseries screening, and standardized flux selection, ensuring transparent processing and minimizing subjective biases (Minaudo et al., 2025). Spatially, the highly localized nature of chamber measurements might derive into large variability of wetland-level average fluxes. This was accounted for by the stratified sampling design, ensuring good representation of relevant strata while allowing for the detection of strata-specific effects. Nevertheless, while the employment of modular chambers allowed for coverage of most strata, their dimensions precluded the sampling of large (>1.5 m) vegetation stands, likely resulting in underestimations of CO₂ uptake for reed dominated sites. Temporally, sampling was limited to one low-tide event per season and relied on opaque chambers instead of direct nighttime measurements. Accordingly, the approach was not intended to generate fully scalable site-level GHG budgets, but to enable consistent and unbiased comparisons across conservation statuses to assess the effects of wetland alteration and restoration on GHG exchanges and climate mitigation potential.

3. Results

3.1. Fluxes across preserved wetlands

Daily net fluxes at preserved sites varied among case pilot wetlands and GHG species (**Figure 2**). Preserved sites generally exhibited daily CO₂ fluxes (mmol CO₂ m⁻² d⁻¹) centred around zero but with substantial variability (**Figure 2a**). Atlantic tidal sites DU (median = -23.2, IQR = -214 to 16.7) and RI (median = -32.4, IQR = -55.7 to -18.2), showed net CO₂ uptake, with DU presenting one of the largest flux variabilities. Mediterranean sites exhibited similarly high variability, with CA showing the highest CO₂ flux (median = 16.7, IQR = -56.7 to 85.3) and VA having CO₂ fluxes closest to net zero (median = 2.0, IQR = -30.2 to 66.1). Eastern sites showed similar CO₂ flux profiles, with intermediate median fluxes and relatively low variability for DA (median = 6.07, IQR = -4.82 to 24.4) and slightly higher fluxes for CU (median = 9.1, IQR = -0.8 to 35.4).

Net daily CH₄ fluxes (mmol CH₄ m⁻² d⁻¹) were generally positive across all preserved sites, with higher median emissions associated with greater variability and strongly skewed distributions (**Figure 2b**). Atlantic tidal wetlands showed the lowest CH₄ emissions, with similar values at DU (median = 1.5×10^{-3} , IQR = -4.2×10^{-3} to 1.6×10^{-2}) and RI (median = 8.3×10^{-3} , IQR = 4.4×10^{-3} to 1.2×10^{-2}). Mediterranean preserved sites exhibited intermediate CH₄ emissions, with CA (median = 1.7×10^{-2} , IQR = 1.8×10^{-3} to 1.5×10^{-1}) showing lower median fluxes than VA (median = 3.4×10^{-2} , IQR = 3.4×10^{-2} to 1.4×10^{-1}) but comparable variability. Eastern preserved sites showed the highest emissions, with DA (median = 1.1, IQR = 0.7 to 9.9) displaying the highest CH₄ fluxes and extreme skewness, while CU (median = 0.8, IQR = 0.4 to 1.7) had lower and less variable CH₄ fluxes.

The contrasting CO₂ and CH₄ flux profiles at preserved sites resulted in CO₂-eq distributions reflecting the dominant contributor to climatic forcing in each case pilot (**Figure 2c**). CO₂ generally dominated the CO₂-eq balance, with CH₄ contributing minor proportions (mean ± SD) in Atlantic (2 ± 5% in both DU and RI) and Mediterranean (8 ± 19 in CA, 7 ± 17 in VA) sites, but substantially higher shares in eastern wetlands (50 ± 32% in DA, 35 ± 27% in CU). Regarding CO₂-eq fluxes (g CO₂ eq. m⁻² d⁻¹), values were lowest in the Atlantic tidal wetlands RI (median = -1.5, IQR = -2.5 to -0.9) and DU (median = -1.0, IQR = -8.9 to 0.7), intermediate in the Mediterranean wetlands VA (median = 0.3, IQR = -1 to 3.1) and CA (median = 0.8, IQR = -1.3 to 4.2) with ranges spanning net zero, and highest in the eastern wetlands CU (median = 0.9, IQR = 0.3 to 2.3) and DA (median = 1, IQR = 0.2 to 3.8) with ranges above net zero.

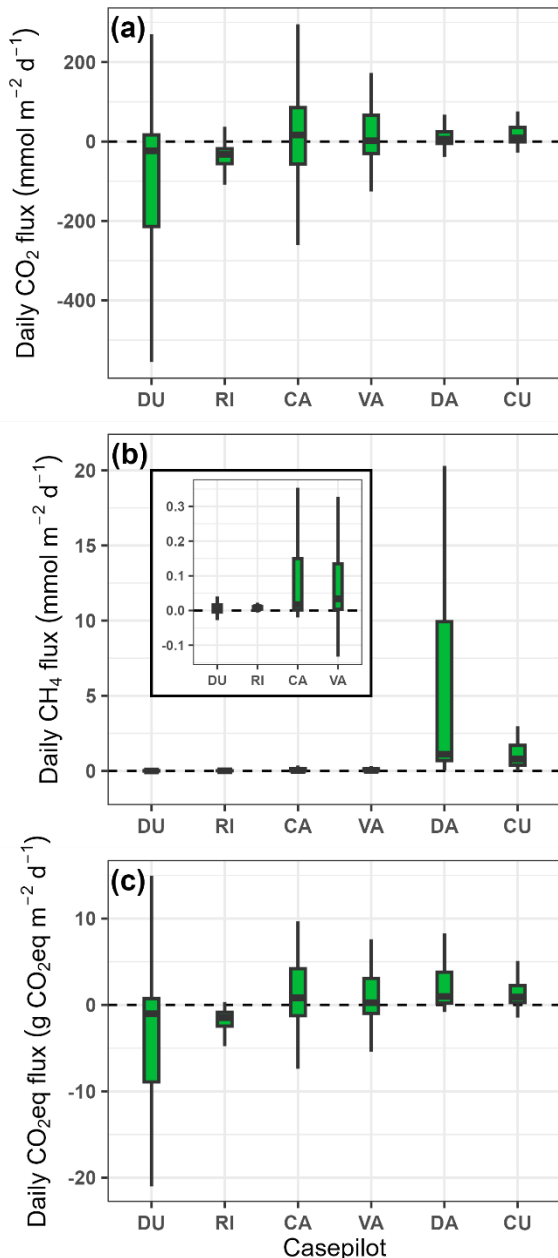


Figure 2. Daily fluxes across preserved case pilot wetlands of (a) CO₂, (b) CH₄, and (c) combined CO₂-eq. Boxplots show the median, interquartile range (IQR), and whiskers extending to 1.5xIQR; potential outliers (data outside the previously defined ranges) are not displayed for clarity. Inset in (b) shows a zoomed-in view of CH₄ flux data for DU, RI, CA, and VA to better visualize differences; y-axis scale differs from the main panel.

3.2. Effect of conservation status on CO₂ fluxes

Daily CO₂ fluxes (mmol m⁻² d⁻¹) showed wetland-specific patterns related to the conservation status (**Figure 3**). Significant status effects were detected in three case pilot wetlands (RI, DA, CU) (**Table S1**), with clear differences between preserved, altered, and restored sites (**Table S3**). In RI and DA, altered sites exhibited significantly higher CO₂ fluxes than preserved ($p \leq 0.004$) and restored ($p < 0.001$) sites, which showed similar low fluxes ($p \geq 0.81$). In contrast, CU displayed lower CO₂ fluxes in altered sites compared to preserved ($p < 0.001$) and restored ($p < 0.001$) sites. No statistically significant status effects were observed in DU, CA, or VA, where CO₂ fluxes were comparable across conservation statuses. Beyond status, CO₂ fluxes were consistently influenced by seasonality and vegetation presence, often interacting with the conservation status, even when status alone was not significant (**Table S1, Figures S3 and S6**).

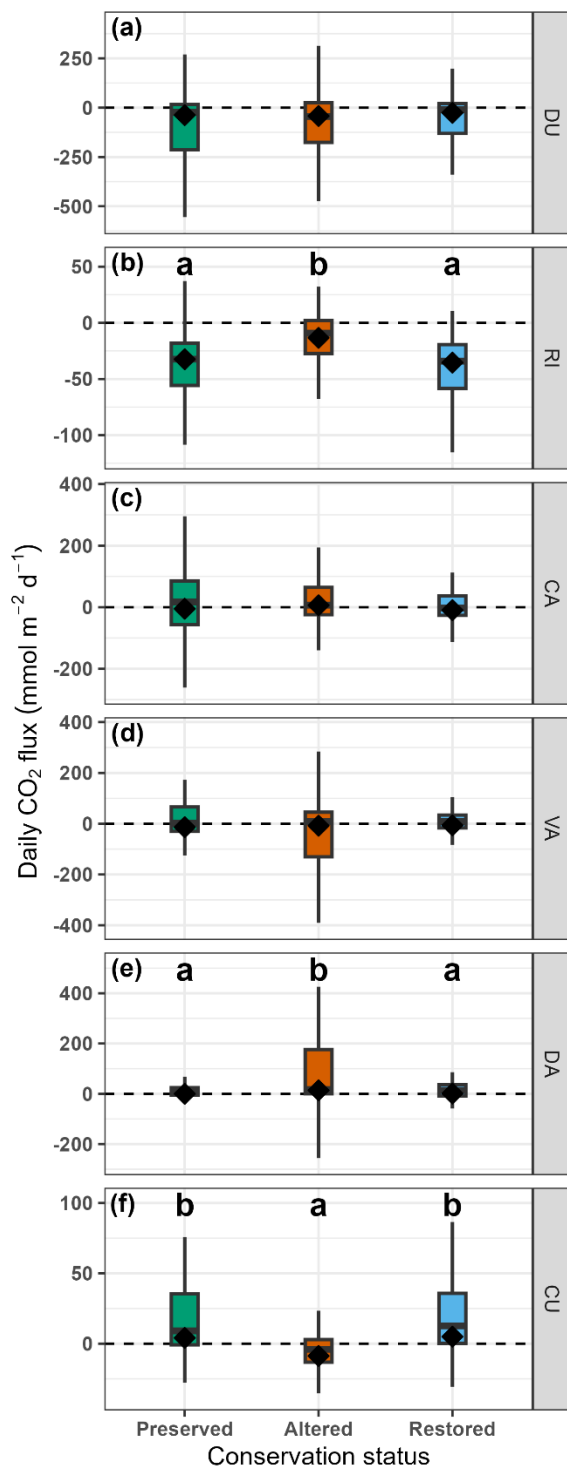


Figure 3. Daily CO₂ fluxes (mmol m⁻² d⁻¹) according to conservation status for each case pilot wetland. Boxplots show the median, interquartile range (IQR), and whiskers extending to 1.5xIQR; potential outliers (data outside the previously defined ranges) are not displayed for clarity. Diamonds represent GLMM-derived EMMs and letters are shown in panels with significantly distinct EMMs groups ($p < 0.05$, post-hoc t-test or z-test, **Table S3**) alphabetically ordered according to group ranks.

3.3. Effect of conservation status on CH₄ fluxes

CH₄ fluxes (mmol m⁻² d⁻¹) showed clearer and more consistent responses to conservation status across case pilot wetlands (**Figure 4**). Significant status effects were detected in all case pilot wetlands except DU (**Table S1**), where CH₄ fluxes did not differ among preserved,

altered and restored sites (**Table S3**). In RI, preserved and restored sites exhibited slightly higher CH₄ fluxes than altered sites ($p = 0.004$, and $p < 0.001$, respectively). In the Mediterranean wetlands (CA and VA), altered sites showed higher CH₄ emissions than preserved sites ($p \leq 0.041$), with restored sites displaying intermediate fluxes. In DA, restored sites had higher CH₄ fluxes than altered sites ($p = 0.044$), while preserved sites were intermediate. In CU, altered sites exhibited substantially higher CH₄ emissions than both preserved ($p = 0.002$) and restored ($p = 0.004$) sites, which showed similarly low fluxes. As for CO₂, CH₄ flux variability was strongly influenced by seasonality across all case pilots and by vegetation presence in most cases, with frequent interactions between the conservation status, season, and vegetation presence (**Table S1; Figure S4 and S7**).

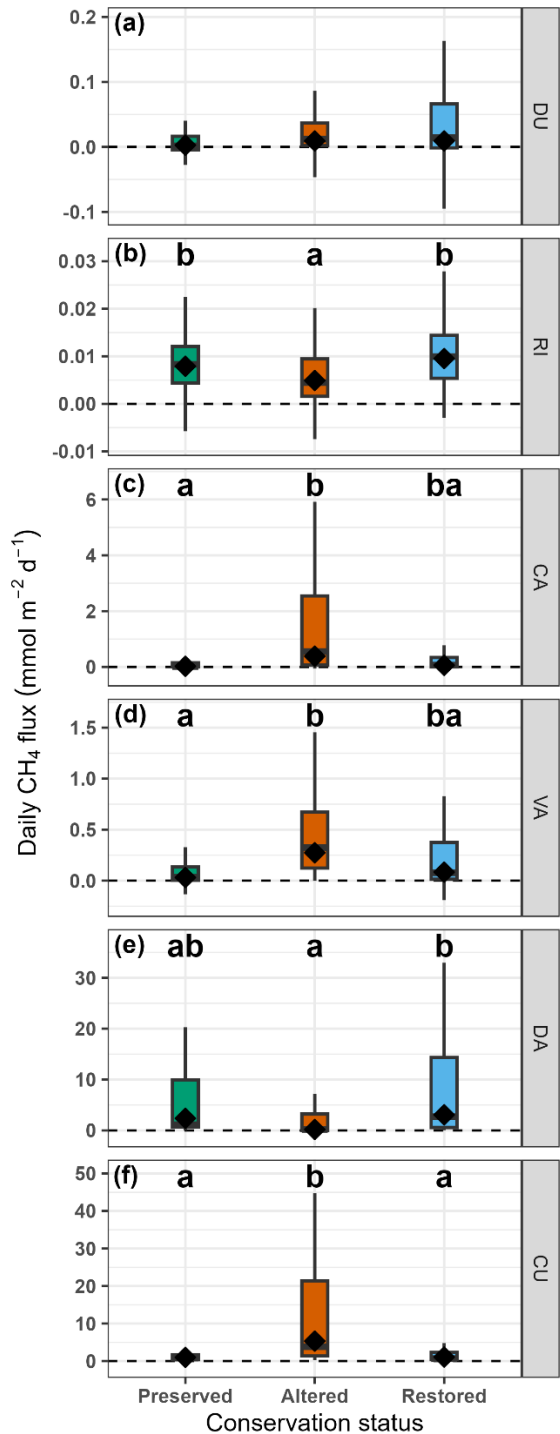


Figure 4. Daily CH₄ fluxes (mmol m⁻² d⁻¹) according to conservation status for each case pilot. Boxplots show the median, interquartile range (IQR), and whiskers extending to 1.5xIQR; potential outliers (data outside the previously defined ranges) are not displayed for clarity. Diamonds represent GLMM-derived EMMs and letters are shown in panels with significantly distinct EMMs groups ($p < 0.05$, post-hoc t.test or z.test, **Table S3**) alphabetically ordered according to group ranks.

3.4. Effect of conservation status on CO₂-eq fluxes

The effects of the conservation status on combined CO₂-eq fluxes (**Figure 5**) were less consistent than for CO₂ and CH₄ alone. Significant status effects were detected in RI, CA, DA and CU (**Table S1**), with significant differences among altered, preserved and restored locations in RI, CA and CU (**Table S3**). No statistically significant status effect was observed in DU and VA ($p \geq 0.76$), where CO₂-eq fluxes were similar across preserved, altered, and restored sites. In RI and CU, preserved and restored sites showed comparable CO₂-eq fluxes ($p \geq 0.34$) that were lower than those of altered sites ($p \leq 0.046$). In CA, preserved sites had lower CO₂-eq fluxes than altered sites ($p = 0.018$), with restored sites showing intermediate values. Although DA showed a significant overall status effect, differences among estimated marginal means were not significant. Across case pilots, seasonality and vegetation presence strongly influenced CO₂-eq fluxes and frequently interacted with the conservation status where status effects were present (**Table S1, Figure S5, Figure S8**).

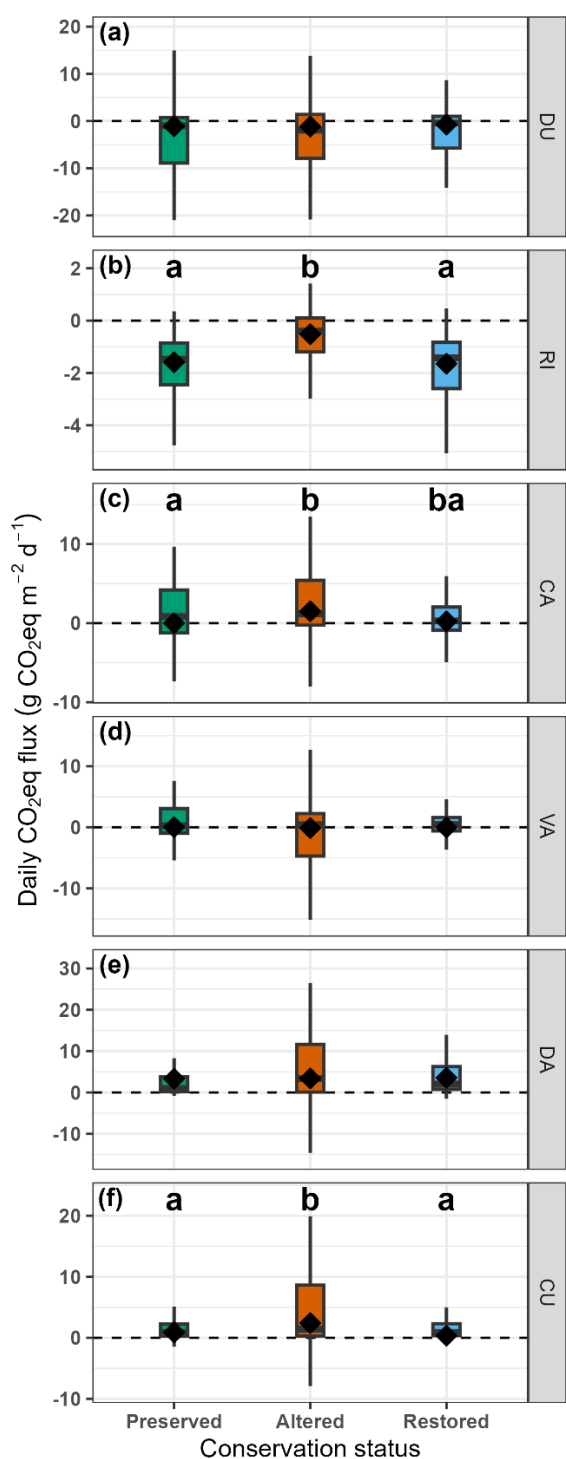


Figure 5. Daily CO₂-eq flux (g CO₂ eq. m⁻² d⁻¹) according to conservation status for each case pilot wetland. Boxplots show the median, interquartile range (IQR), and whiskers extending to 1.5xIQR; potential outliers (data outside the previously defined ranges) are not displayed for clarity. Diamonds represent GLMM-derived EMMs and letters are shown in panels with significantly distinct EMMs groups ($p < 0.05$, post-hoc t.test or z.test, **Table S3**) alphabetically ordered according to group ranks.

4. Discussion

4.1. Biogeochemical drivers of gaseous C exchange in European coastal wetlands

Across the wetlands examined, the effects of conservation status on CO₂, CH₄ fluxes varied among the studied wetland types, main types of alterations and associated restoration measures. CO₂ fluxes showed variations associated with the conservation status in only three of six case pilots, whereas CH₄ fluxes were more responsive, with significant effects in five of six case pilots. Wherever status effects were detected for CO₂, they were consistently opposite in direction to those of CH₄, reflecting contrasting conditions that control the underlying processes regulating CO₂ and CH₄ exchanges in the different wetlands considered, with enhancement of aerobic conditions increasing CO₂ release, while actions favoring anaerobic conditions (e.g., rewetting) increased CH₄ emissions. Despite this variability, mostly depending on the specific features of each wetland type and the conservation status of sites, some common mechanisms were evident across wetland types.

The diversity of wetland types and ecological conditions examined allowed identification of key drivers of CO₂ and CH₄ exchanges, strongly modulated by seasonality. CO₂ fluxes were primarily controlled by vegetation cover and sediment oxygen availability, which regulated the balance between photosynthetic uptake and respiration-mediated release of CO₂. Emissions of CH₄ were mostly related to hydrology-driven oxygen availability in the sediment, salinity conditions, and presence of reed-type vegetation, with labile organic matter supply being important in some systems. CO₂ exchange responded mostly to alteration and restoration actions that severely modified the landscape of the wetlands, either through substantial loss or gain in abundance of primary producers or through profound changes in inundation patterns related to land-use change. CH₄ emissions were more sensitive to subtler hydrological changes, either through variations in water quality and salinity or through hydrodynamics modifying the extent and timing of wetlands flooding and water table depths. This sensitivity is strongly seasonal and temperature-driven, an effect that becomes increasingly evident at lower latitudes. Global changes that extend warm periods could potentially extend the duration of the observed seasonal CH₄ emission peaks in summer (Camacho et al., 2017; Morant et al., 2024); thus, accounting for seasonal variability is essential to accurately assess restoration outcomes, or the consequences of their absence.

Emergent vegetation presence exerted strong and consistent impact on CO₂ fluxes across all wetland types where it was evaluated, with vegetated areas generally acting as net CO₂ sinks (**Table S1; Figure S6**). This evidences that, although strongly regulated by seasonality and local climatic conditions, vegetation standing stock is a primary driver of ecosystem-level primary production through photosynthetic uptake of CO₂ (Reddy et al., 2022). While our statistical framework could not explicitly include this effect for the seagrass meadows of Ria de Aveiro, the expected stronger CO₂ uptake by *Zostera noltii* meadows with respect to bare mudflats becomes evident when considering the strong differences in vegetated coverage between the sites of different conservation status sampled. RI altered sites suffered from erosion, bait-digging and trampling (**Table 1**), which reduced their *Z. noltii* coverage to an average of 8%. Instead, preserved sites as well as restored sites after

seagrass planting showed much higher average *Z. noltii* coverages (61% and 96%, respectively), which is the likely explanation behind the significantly enhanced CO₂ uptake shown by these sites (**Figure 3b**).

Plant community composition is also sometimes shown to influence overall CO₂ uptake rates in wetlands (Ward et al., 2009). Several of the wetlands studied suffered from alterations that involved modified vegetation communities such as presence of invasive species and loss of native vegetation and land use change (**Table 1**). Generally, the CO₂ exchange profile in vegetated areas of different conservation status did not reveal significant differences (**Figure S6**), indicating that environmental alterations related to shifts in plant community composition had little impact on CO₂ exchange in the studied wetlands. While vegetation composition is a good indicator of the overall ecological integrity of wetland systems, the potential biogeochemical effects of these types of shifts (Davidson et al., 2018) were not of sufficient magnitude to be detected in our study. Although the vegetated areas of the Danube Delta wetlands did show significant differences that might be associated with differences in primary productivity of reed stands and agricultural crop species (**Figure S6**), these coincided with permanently inundated substrates and agricultural soils, respectively. Thus, the observed differences likely arise from two main factors: differences in vegetation primary production efficiency and lower aerobic respiration rates due to oxygen limitation in submerged sediments and the water column compared with well-aerated agricultural soils (Bianchi et al., 2021). This interpretation is supported by the higher CO₂ emissions measured in non-vegetated areas of altered sites relative to preserved and restored sites in the Danube Delta (**Figure S6**). These two non-exclusive mechanisms likely resulted in the status-level differences in CO₂ fluxes observed in the Danube Delta (**Figure 3e**). Finally, the abundance of other primary producers (phytoplankton) appears to be the dominant driver responsible for the CO₂ exchange profiles observed in the Curonian Lagoon (**Figure 3f**). In this wetland, nutrient load was the main alteration factor related to conservation status and ecosystem interventions (**Table 1**), leading to eutrophication and associated massive phytoplankton blooms in altered sites (Vaičiūtė et al., 2021; Zilius et al., 2013), as indicated by water chlorophyll-*a* concentrations (**Table S4**). Thus, enhanced CO₂ uptake and reduced respiration under anoxic conditions driven by organic C accumulation by phytoplankton in open water areas (**Figure S6**) seem to be the main drivers behind the general status-level differences in CO₂ exchange profiles of the Curonian Lagoon (**Figure 3f**).

Hydrology emerged as a dominant control on CH₄ exchanges across the wetlands studied. Permanently flooded sediments promote anoxic conditions that favor methanogenesis (Camacho-Santamans et al., 2025; Rochera et al., 2025b) while restricting aerobic respiration and thus CO₂ releases. This mechanism is exemplified by the general inter-wetland type variability observed for CH₄ (**Figure 2**), where freshwater systems characterized by permanently flooded conditions, where salinity does not control methanogenesis (Camacho et al., 2017; Miralles-Lorenzo et al., 2025; Morant et al., 2024), such as Danube Delta lakes and the Curonian Lagoon, present by far the largest emission profiles of CH₄. A similar pattern was observed for the freshwater marshes of Camargue, where wetland hydrology was a main determinant of the conservation status (**Table 1**) and CH₄ emissions (**Figure 4c**). CA altered sites hydrodynamics favored flooded conditions, as reflected by 73 % of chamber deployments in these sites occurring in inundated areas with respect to 48% for preserved sites. Accordingly, altered sites presented overall higher CH₄ emissions (**Figure 4c, Table S3**), particularly during the summer season (**Figure S4**),

coinciding with highest discrepancy in flooded area proportion between altered and preserved sites (82% vs. 40%) and high temperatures that likely limited oxygen availability and enhanced microbial activity in submerged sediments (Cui et al., 2024). Modified hydrology was also an important factor regulating CH₄ emissions in the brackish Mediterranean marshes of Marjal dels Moros, where similar patterns in inundation proportion (65% vs 26%) were likely contributing to the higher CH₄ emissions observed in altered sites, with respect to preserved ones (**Figure 4d**).

Nevertheless, CH₄ emissions were not only influenced by hydrology-driven oxygen availability of the sediments but also by another of the main regulating factors of CH₄ production in coastal wetlands, namely salinity. Through the provision of sulfate as a more energetically favorable electron acceptor than CO₂, seawater intrusion regulates the dominance of sulfate-reducing over methanogenic microbes (Koebsch et al., 2019; (Miralles-Lorenzo et al., 2025). This mechanism helps to explain the gradient in CH₄ emissions observed along the progressively more saline altered, restored and preserved sites of Marjal dels Moros (**Figure 4d, Table S4**). Additionally, this salinity-driven methanogenesis limitation in tidal wetlands such as DU saltmarshes and RI *Z. noltii* meadows is likely responsible for their extremely low CH₄ emissions with respect to the other coastal wetlands examined (**Figure 2**).

While anoxia and salinity help to regulate the dominant catabolic metabolism in sediments, the supply of different organic matter substrates is one of the principal factors regulating the overall rates of organic C degradation, and CH₄ emissions (Rissanen et al., 2023). Across the wetlands examined, the effect of labile organic matter supply in regulating CH₄ production can help to explain small but significantly higher CH₄ emissions of preserved and restored *Z. noltii* meadows with respect to bare altered sites of RI (**Figure 4b**), as seagrasses produce and release methylated compounds that represent an attractive substrate for methanogens (Schorn et al., 2022). Of more relevance is the pattern observed in the Curonian Lagoon wetland, where enhanced phytoplankton growth fueled by increased nutrient loads (**Table S4**) resulted in an accumulation of labile organic matter in the sediments of altered sites (Remeikaite-Nikiene et al., 2016). Rapid degradation of phytoplankton-derived organic-C leads to anoxic conditions which, together with the freshwater character of the sites (Zilius et al., 2013), resulted in an ideal environment for methanogenesis, helping to explain the stark differences in CH₄ overall emissions between the altered and preserved and restored sites of this wetland (**Figure 4f**). Additionally, although these increased emissions of CU eutrophic sites were consistently detected in both open-water and vegetated areas, the magnitude of CH₄ emissions was much higher in reed-covered zones of CU, which is a common pattern observed across many of the wetlands examined (**Figure S7**). The consistently higher CH₄ emissions observed in vegetated zones likely result from vegetation-facilitated transfer of CH₄ from sediments to the atmosphere, bypassing oxidation in sediments and the water column (Ge et al., 2024). However, this enhanced CH₄ release generally does not exceed photosynthetic C assimilation when assessed in terms of net C balance.

Across wetlands, two non-exclusive mechanisms emerged as primary drivers of changes in GHG exchange: shifts in areal habitat composition and changes in process rates within habitats. Major alterations and restoration actions can modify wetland structure to the point where entire habitats are lost along with their biogeochemical functioning. The loss and replantation of seagrass beds in Ria de Aveiro or the land-use changes of the Danube

Delta wetlands are extreme examples of this mechanism. Conversely, subtler interventions that do not visually alter the ecosystem landscape can nonetheless shift underlying processes and result in significant impacts on biogeochemical process rates. The degradation and subsequent recovery of water quality in the Curonian Lagoon through regulation of nutrient-loads is a good example for this process: while the composition of open water and reed beds habitats remained the same between altered and restored sites, their habitat-specific rates of CO₂ and CH₄ production and atmospheric exchange were significantly different (**Figures S6, S7**). While the above examples represent extremes of these two mechanisms, it is important to recognize the existence of a continuum between them. It is also important to acknowledge that no single habitat-specific “reference” rate exists for any natural process. In this context, seasonal variability regulates GHG fluxes through two pathways: temperature and physiological shifts alter habitat-specific process rates, while seasonal flooding dynamically redistributes the relative extent of open water, vegetated areas, and bare sediments within wetlands.

The contrasting sensitivities and drivers of CO₂ and CH₄ often led to opposite flux responses to the same environmental interventions, making CO₂-eq outcomes dependent on wetland-specific gas dominance. Three general response groups emerged. In tidal wetlands (Dutch Delta and Ria de Aveiro), constant seawater supply suppressed CH₄ emissions to the point that this gas only represented an average 3% and 2% of CO₂-eq exchanges, respectively. In these wetlands, only vegetation-related interventions resulted in a significant impact on their climatic functionality, with changes in CO₂ fluxes outbalancing all detected variations in CH₄ emissions. In seasonally inundated Mediterranean marshes (Camargue and Marjal dels Moros), CH₄ played a moderate role in their CO₂-eq fluxes (18% and 11%, respectively). In these wetlands, CO₂-eq flux changes were detected only when interventions strongly affected CH₄ emissions. In permanently flooded freshwater wetlands (Danube lakes and Curonian Lagoon), CH₄ represented a higher average proportion of the wetland GHG balance in terms of CO₂-eq (43% and 46%, respectively). In these wetlands, ecosystem interventions had clear but opposite effects for CO₂ and CH₄ exchanges, which only resulted in changes of combined CO₂-eq fluxes when CO₂ responses were of relatively low magnitude and outbalanced by strong CH₄ changes.

4.2. Climate change mitigation potential of coastal European wetland restoration and conservation

This study offers valuable insights into the potential of European coastal wetland restoration as a climate mitigation tool through the exemplary results obtained from six diverse pilot wetlands. Comparison of CO₂, CH₄ and CO₂-eq exchange balances between altered and restored sites provide a quantitative estimate of the mitigation capacity of restoration across different wetland types (**Table S3**).

Although the central distributions of daily net fluxes showed apparent reductions in GHG fluxes following restoration in several pilot wetlands (**Figures 3, 4, 5**), driven by significant effects of the conservation status (**Table S1**), high data variability precluded the detection of statistically significant mean flux reductions in some cases (**Table S3**). Across the pilot wetlands, statistically significant mitigation capacity of CO₂ fluxes was only detected for the restoration of Ria de Aveiro seagrass meadows and Danube Delta freshwater lakes, likely driven by increased net primary production of seagrass with respect to bare sediment areas and reduced organic C decomposition rates in freshwater lakes compared with agricultural

land use, respectively. For CH₄ fluxes, statistically significant mitigation was only observed following water quality improvement of the Curonian Lagoon, while restoration of natural hydrodynamics in Camargue achieved marginal CH₄ reductions that approached statistical significance. When CO₂ and CH₄ were combined as CO₂-eq, statistically significant mitigation potential was statistically significant only for seagrass replantation in Ria de Aveiro and re-oligotrophication in the Curonian Lagoon.

The results show mitigation potential for restoration of some types of degraded coastal European wetlands; however, the cumulative nature of GHG emissions must be considered. Even in cases where restoration completely reverts the biogeochemical functioning of a degraded wetland back to pristine conditions, the net effect must account for the time during which the wetland presented increased emissions incurring in a “recovery debt” (Moreno-Mateos et al., 2017). While the limited potential impact of restoration might appear discouraging, the same temporal consideration highlights the elevated and persistent costs of inaction and the necessity to avoid degradation of coastal wetlands in the first place. In fact, considering the differences in GHG profile associated to sites of preserved and degraded conservation status reveals clear trends that demonstrate the high mitigation potential of maintaining coastal European wetlands in good conservation status (**Table S3**). Potentially avoided emissions through conservation were generally of similar or higher magnitude than those associated with restoration and achieved statistical significance in more cases. These patterns reveal fundamental differences in the functioning of well preserved and restored ecosystems.

Restoration projects guided by ecological restoration theory typically focus on alleviating pressures through passive restoration and reconstructing ecosystem structures to accelerate inherent functional recovery via active restoration (Palmer et al. 2016). However, even when restoration is well implemented, functional recovery often lags structural recovery due to slow reestablishment of natural biotic networks underpinning biogeochemical processes (Moreno-Mateos et al., 2012). Additionally, hysteretic dynamics in the face of ecosystem degradation and recovery may lead to trajectories favouring unintended alternative degraded states (Suding et al., 2004). Overall, the risks inherent to wetland restoration, recovery pathways and generally slow biogeochemical functional recovery emphasizes the importance of preserving natural wetlands in a good conservation status.

Despite the differences shown above, conservation and restoration are complementary tools for climate mitigation and should not be viewed as alternative management strategies. It is important to recognise that our current assessment of restoration’s mitigation capacity does not account for other biogeochemically relevant benefits, such as expansion of wetland extent or reductions of nitrous oxide (N₂O) emissions (Kasak et al., 2021; Leo et al., 2019), and represents only a snapshot of the functional recovery process likely to improve over time (Moreno-Mateos et al., 2017). Thus, the lack of statistically significant reductions in areal CO₂ and CH₄ exchanges reported in **Table S3** should not be interpreted as evidence that wetland restoration lacks climate mitigation benefits. Moreover, none of the restoration strategies implemented across the different wetlands examined targeted GHG mitigation as an explicit primary objective (Oliveira et al., under review). Therefore, the detected effects on GHG exchanges can be considered as an additional co-benefit to the impact of restoration in improving other ecosystem services such as biodiversity, water quality and flood risk mitigation (Meli et al., 2014; Singh et al., 2019; Wu et al., 2023). Ultimately,

although the results show that restoration caused significant increases in emissions of either CO₂ or CH₄ in some wetlands, these were always accompanied by similar or greater changes in the opposite direction for the other GHG species studied. Therefore, when considering the overall climatic impacts attributable to restoration, the only significant effects detected for CO₂-eq exchanges were net reductions, indicating the generation of a climatic cooling capacity (**Table S3**).

This study highlights the diverse biogeochemical controls on GHG regulation across European coastal wetlands under different conservation statuses. These functional and site-specific differences must be explicitly considered in restoration and management planning to avoid trade-offs with other ecosystem services (Pörtner et al., 2021). Restoration strategies should therefore incorporate targeted, long-term monitoring to track wetland recovery and detect structural or functional deviations that require corrective action.

Wetlands have been heavily impacted by land-use change due to the historical undervaluation of their ecosystem services, often favouring higher-value uses despite substantial ecological losses (Zorrilla-Miras et al., 2014). This underscores the need to explore financing mechanisms that recognize the economic value of wetland ecosystem services, particularly their potential for climate mitigation. However, wetland climate mitigation capacity arises from complex, system-specific interactions among multiple GHGs, characterized by high spatial and temporal variability. Financing schemes should therefore be linked to comprehensive, long-term monitoring of all relevant GHG fluxes to avoid incomplete accounting and over-crediting risks prevalent in current carbon offset markets (Romm et al., 2025). Ultimately, for coastal wetland restoration to be an effective nature-based climate solution, projects must demonstrate additionality, feasibility, and permanence, and provide enough evidence to accurately quantify their climate benefits (Jones et al., 2024).

Currently, estimates of climate mitigation capacity of wetland restoration are highly variable (Griscom et al., 2017), stemming from incomplete understanding of several climate relevant processes. A common identified issue is the lack of widespread data on how GHG exchanges, in particular CH₄ and N₂O emissions, respond to coastal wetland restoration (Rosentreter et al., 2021). While the climatic effect of restoration projects in other ecosystems might be well represented by simple C balance assessments, in wetlands systems monitoring of these non-CO₂ GHG exchanges is essential to accurately quantify net climatic impact (Macreadie et al., 2019). Transient increases in CH₄ emissions from restored wetlands can, considering radiative forcings and atmospheric lifetimes of GHGs, considerably delay climatic benefits of increased C storage (Schuster et al., 2024). Therefore, wetland restoration actions that achieve timely reductions of CH₄ emissions, such as those of Curonian Lagoon and to a lesser extent Camargue and Marjal dels Moros, become especially relevant to meet climatic mitigation targets. Additionally, the importance of lateral C and off-site GHG exchanges is increasingly being recognized, and future studies should therefore aim to obtain a more complete assessment of watershed-level budgets that support management decisions (Jones et al., 2024; Regnier et al., 2022). Finally, appropriate pre-restoration baseline reference conditions measurements are essential to provide actionable knowledge to managers, thereby allowing quantification of actual benefits of alteration-specific reversals.

680 Given the ample and clear benefits of coastal wetland restoration on the provisioning of
681 other ecosystem services, widespread restoration of degraded systems should
682 nonetheless be pursued. We advocate to taking advantage of recent policy momentum,
683 exemplified by the EU Nature Restoration Regulation, to gather more evidence on the
684 effects of coastal wetland restoration on GHG regulation, enabling us to quantify more
685 precisely the magnitude, consistency and reliability of associated climatic benefits.

5. Conclusions

This study examined how the conservation status and restoration of diverse European coastal wetlands influence atmospheric exchanges of CO₂ and CH₄ and their combined effects on climate forcing expressed as CO₂eq. The results of this study show that GHG fluxes respond differently to degradation and restoration actions depending on the wetland type and associated main biogeochemical drivers. In particular, CO₂ fluxes responded primarily to landscape-scale changes in vegetation cover and inundation, whereas CH₄ exchanges were more sensitive to environmental modification and readily responded to comparatively subtle changes in water quality, salinity, and hydrodynamics.

These contrasting responses, joined with different relative contributions of CO₂ and CH₄ to net climatic forcing, translated into wetland-specific CO₂eq mitigation potentials associated with restoration and conservation. Replantation of seagrass meadows and eutrophication reversal through improved water treatment emerged as effective restoration measures for increasing climate mitigation capacity of degraded wetlands. Other actions, such as the reestablishment of natural salinity and hydrodynamics regimes showed signs of reducing CH₄ emissions, but high CO₂ flux variability precluded detection of significant reductions in combined CO₂-eq emissions with the measured data.

While this study did not assess potential changes in N₂O emissions, the observed patterns for CO₂ and CH₄ contribute to the growing body of evidence supporting wetland restoration as an effective nature-based solution for climate change mitigation. At the same time, the findings of our study underscore the importance of considering multiple GHG and their specific biogeochemistry when evaluating the climatic impact of wetland restoration projects. Further research should therefore aim to simultaneously quantify exchanges of CO₂, CH₄ and N₂O over management-relevant timeframes to better characterize the functional recovery process and obtain more complete assessments of the climatic benefits associated to wetland restoration.

Within the scope of this study, restoration projects implemented across a range of European coastal wetland types showed no evidence of significant detrimental effects in terms of CO₂eq. Instead, the results demonstrate that restoration can enhance or, at minimum, maintain climate regulation functions. Joined with ample evidence for other ecosystem service co-benefits, the results of our study support current regulatory efforts aimed at recovering historically degraded European wetlands while underscoring the need for targeted, ecosystem-specific restoration strategies to maximize climate mitigation potential.

Acknowledgments

Funding for this research came from the project RESTORE4Cs - *Modelling RESTORation of wEtlands for Carbon pathways, Climate Change mitigation and adaptation, ecosystem services, and biodiversity, Co-benefits* (DOI: 10.3030/101056782), funded by the European Union under the Horizon Europe research and innovation programme (Grant Agreement ID: 101056782). The views and opinions expressed are those of the author(s) only and do not necessarily reflect those of the European Union or the granting authority. Neither the European Union nor the granting authority can be held responsible for them. We also acknowledge the support of FCT – Fundação para a Ciência e a Tecnologia I.P., to CESAM-Centro de Estudos do Ambiente e do Mar, under the project references UID/50017/2025 (doi.org/10.54499/UID/50017/2025) and LA/P/0094/2020 (doi.org/10.54499/LA/P/0094/2020). We thank Ana Ribeiro for logistical support. Work by the University of Valencia was also co-supported by projects CLIMAWET-CONS (PID2019-104742RB-I00), funded by the Agencia Estatal de Investigación of the Spanish Government, and by the project ECCAEL (PROMETEO CIPROM-2023-031), funded by the Generalitat Valenciana, both granted to Antonio Camacho.

Declaration of generative AI and AI-assisted technologies in the manuscript preparation process

During the preparation of this work the authors used ChatGPT-5.2 in order to identify potential improvements in text readability and for coding syntax support during data processing. After using this tool/service, the authors reviewed and edited the content as needed and take full responsibility for the content of the published article.

Data and code availability

Data presented in this article is deposited at LifeWatch ERIC (<https://doi.org/10.48372/C29B-QW38>) and will be fully accessible after December 31st, 2027. During embargo period, data will be made available upon reasonable request. Code to reproduce results of this article is fully accessible at: https://github.com/MCabreraBrufau/CabreraBrufau_et_al_2026_code.

References

- Airolidi, L., Beck, M., 2007. Loss, status and trends for coastal marine habitats of Europe, in: Gibson, R.N., Atkinson, R.J.A., Gordon, J.D.M. (Eds.), *Oceanography and Marine Biology: An Annual Review*. CRC Press, pp. 1–566. <https://doi.org/10.1201/9781420050943>
- Bertolini, C., da Mosto, J., 2021. Restoring for the climate: a review of coastal wetland restoration research in the last 30 years. *Restor Ecol* 29, e13438. <https://doi.org/10.1111/rec.13438>
- Bianchi, A., Larmola, T., Kekkonen, H., Saarnio, S., Lång, K., 2021. Review of Greenhouse Gas Emissions from Rewetted Agricultural Soils. *Wetlands* 2021 41:8 41, 108-. <https://doi.org/10.1007/S13157-021-01507-5>
- Bonaglia, S., Cheung, H.L.S., Politi, T., Vybernaite-Lubiene, I., McKenzie, T., Santos, I.R., Zilius, M., 2025. Eutrophication and urbanization enhance methane emissions from coastal lagoons. *Limnol Oceanogr Lett* 10, 140–150. <https://doi.org/10.1002/lol2.10430>
- Cabrera-Brufau, M., Minaudo, C., von Schiller, D., Obrador, B., Attermeyer, K., Camacho, A., 2025. Instantaneous fluxes of carbon dioxide (CO₂) and methane (CH₄) of six European coastal wetlands under different ecological status measured seasonally with static chambers [Data set]. LifeWatch ERIC. <https://doi.org/10.48372/C29B-QW38>
- Camacho, A., Picazo, A., Rochera, C., Santamans, A., Morant, D., Miralles-Lorenzo, J., Castillo-Escrivà, A., 2017. Methane Emissions in Spanish Saline Lakes: Current Rates, Temperature and Salinity Responses, and Evolution under Different Climate Change Scenarios. *Water (Basel)* 9, 659. <https://doi.org/10.3390/w9090659>
- Camacho-Santamans, A., Morant, D., Rochera, C., Picazo, A., Camacho, A., 2025. Towards an enhancement of the climate change mitigation capacity of inland saline shallow lakes through hydrological regime and vegetation management: a modelling approach. *Water Int* 50, 197–224. <https://doi.org/10.1080/02508060.2024.2311997>
- Canadell, J.G., Monteiro, P.M.S., 2023. Global Carbon and Other Biogeochemical Cycles and Feedbacks, in: *Climate Change 2021 – The Physical Science Basis*. Cambridge University Press, pp. 673–816. <https://doi.org/10.1017/9781009157896.007>
- Cui, S., Liu, P., Guo, H., Nielsen, C.K., Pullens, J.W.M., Chen, Q., Pugliese, L., Wu, S., 2024. Wetland hydrological dynamics and methane emissions. *Communications Earth & Environment* 2024 5:1 5, 470-. <https://doi.org/10.1038/s43247-024-01635-w>
- Davidson, I.C., Cott, G.M., Devaney, J.L., Simkanin, C., 2018. Differential effects of biological invasions on coastal blue carbon: A global review and meta-analysis. *Glob Chang Biol* 24, 5218–5230. <https://doi.org/10.1111/gcb.14426>
- European Environment Agency, 2024. Europe's state of water 2024 – The need for improved water resilience. Publications Office of the European Union. <https://doi.org/doi/10.2800/02236>

European Union, 2024. Regulation (EU) 2024/1991 of the European Parliament and of the Council of 24 June 2024 on nature restoration and amending Regulation (EU) 2022/869.

Fluet-Chouinard, E., Stocker, B.D., Zhang, Z., Malhotra, A., Melton, J.R., Poulter, B., Kaplan, J.O., Goldewijk, K.K., Siebert, S., Minayeva, T., Hugelius, G., Joosten, H., Barthelmes, A., Prigent, C., Aires, F., Hoyt, A.M., Davidson, N., Finlayson, C.M., Lehner, B., Jackson, R.B., McIntyre, P.B., 2023. Extensive global wetland loss over the past three centuries. *Nature* 2023 614:7947 614, 281–286. <https://doi.org/10.1038/s41586-022-05572-6>

Ge, M., Korrensalo, A., Laiho, R., Kohl, L., Lohila, A., Pihlatie, M., Li, X., Laine, A.M., Anttila, J., Putkinen, A., Wang, W., Koskinen, M., 2024. Plant-mediated CH₄ exchange in wetlands: A review of mechanisms and measurement methods with implications for modelling. *Science of the Total Environment*. <https://doi.org/10.1016/j.scitotenv.2023.169662>

Graves, S., Piepho, H.-P., with help from Sundar Dorai-Raj, L.S., 2024. multcompView: Visualizations of Paired Comparisons. <https://doi.org/10.32614/CRAN.package.multcompView>

Griscom, B.W., Adams, J., Ellis, P.W., Houghton, R.A., Lomax, G., Miteva, D.A., Schlesinger, W.H., Shoch, D., Siikamäki, J. V., Smith, P., Woodbury, P., Zganjar, C., Blackman, A., Campari, J., Conant, R.T., Delgado, C., Elias, P., Gopalakrishna, T., Hamsik, M.R., Herrero, M., Kiesecker, J., Landis, E., Laestadius, L., Leavitt, S.M., Minnemeyer, S., Polasky, S., Potapov, P., Putz, F.E., Sanderman, J., Silvius, M., Wollenberg, E., Fargione, J., 2017. Natural climate solutions. *Proceedings of the National Academy of Sciences* 114, 11645–11650. <https://doi.org/10.1073/pnas.1710465114>

Hartig, F., 2024. DHARMA: Residual Diagnostics for Hierarchical (Multi-Level / Mixed) Regression Models. <https://doi.org/10.32614/CRAN.package.DHARMA>

He, T., Ding, W., Cheng, X., Cai, Y., Zhang, Y., Xia, H., Wang, X., Zhang, J., Zhang, K., Zhang, Q., 2024. Meta-analysis shows the impacts of ecological restoration on greenhouse gas emissions. *Nat Commun* 15, 2668. <https://doi.org/10.1038/s41467-024-46991-5>

Hutchinson, G.L., Mosier, A.R., 1981. Improved Soil Cover Method for Field Measurement of Nitrous Oxide Fluxes. *Soil Science Society of America Journal* 45, 311–316. <https://doi.org/10.2136/sssaj1981.03615995004500020017x>

IPCC, 2023. Climate Change 2021 – The Physical Science Basis. Cambridge University Press, Cambridge. <https://doi.org/10.1017/9781009157896>

Jones, S.F., Arias-Ortiz, A., Baldocchi, D., Eagle, M., Friess, D.A., Gore, C., Noe, G., Nolte, S., Oikawa, P., Paytan, A., Raw, J.L., Roberts, B.J., Rogers, K., Schutte, C., Stagg, C.L., Thorne, K.M., Ward, E.J., Windham-Myers, L., Yando, E.S., 2024. When and where can coastal wetland restoration increase carbon sequestration as a natural climate solution? *Cambridge Prisms: Coastal Futures*. <https://doi.org/10.1017/cft.2024.14>

Kasak, K., Espenberg, M., Anthony, T.L., Tringe, S.G., Valach, A.C., Hemes, K.S., Silver, W.L., Mander, Ü., Kill, K., McNicol, G., Szutu, D., Verfaillie, J., Baldocchi, D.D., 2021. Restoring wetlands on intensive agricultural lands modifies nitrogen cycling microbial

831 communities and reduces N₂O production potential. *J Environ Manage* 299, 113562.
832 <https://doi.org/10.1016/J.JENVMAN.2021.113562>

833 Koebisch, F., Winkel, M., Liebner, S., Liu, B., Westphal, J., Schmiedinger, I., Spitz, A., Gehre,
834 M., Jurasinski, G., Köhler, S., Unger, V., Koch, M., Sachs, T., Böttcher, M.E., 2019.
835 Sulfate deprivation triggers high methane production in a disturbed and rewetted
836 coastal peatland. *Biogeosciences* 16, 1937–1953. [https://doi.org/10.5194/BG-16-](https://doi.org/10.5194/BG-16-1937-2019)
837 [1937-2019](https://doi.org/10.5194/BG-16-1937-2019)

838 Lenth, R. V, 2025. emmeans: Estimated Marginal Means, aka Least-Squares Means.
839 <https://doi.org/10.32614/CRAN.package.emmeans>

840 Leo, K.L., Gillies, C.L., Fitzsimons, J.A., Hale, L.Z., Beck, M.W., 2019. Coastal habitat
841 squeeze: A review of adaptation solutions for saltmarsh, mangrove and beach
842 habitats. *Ocean Coast Manag* 175, 180–190.
843 <https://doi.org/10.1016/J.OCECOAMAN.2019.03.019>

844 Lin, C.W., Lin, W.J., Ho, C.W., Kao, Y.C., Yong, Z.J., Lin, H.J., 2024. Flushing emissions of
845 methane and carbon dioxide from mangrove soils during tidal cycles. *Science of The*
846 *Total Environment* 919, 170768. <https://doi.org/10.1016/J.SCITOTENV.2024.170768>

847 Lorke, A., Bodmer, P., Noss, C., Alshboul, Z., Koschorreck, M., Somlai-Haase, C., Bastviken,
848 D., Flury, S., McGinnis, D.F., Maeck, A., Müller, D., Premke, K., 2015. Technical note:
849 drifting versus anchored flux chambers for measuring greenhouse gas emissions from
850 running waters. *Biogeosciences* 12, 7013–7024. [https://doi.org/10.5194/bg-12-7013-](https://doi.org/10.5194/bg-12-7013-2015)
851 [2015](https://doi.org/10.5194/bg-12-7013-2015)

852 Lovley, D.R., Klug, M.J., 1983. Sulfate reducers can outcompete methanogens at freshwater
853 sulfate concentrations. *Appl Environ Microbiol* 45, 187–192.
854 <https://doi.org/10.1128/AEM.45.1.187-192.1983;WGROU:STRING:PUBLICATION>

855 Macreadie, P.I., Anton, A., Raven, J.A., Beaumont, N., Connolly, R.M., Friess, D.A., Kelleway,
856 J.J., Kennedy, H., Kuwae, T., Lavery, P.S., Lovelock, C.E., Smale, D.A., Apostolaki, E.T.,
857 Atwood, T.B., Baldock, J., Bianchi, T.S., Chmura, G.L., Eyre, B.D., Fourqurean, J.W.,
858 Hall-Spencer, J.M., Huxham, M., Hendriks, I.E., Krause-Jensen, D., Laffoley, D.,
859 Luisetti, T., Marbà, N., Masque, P., McGlathery, K.J., Megonigal, J.P., Murdiyarso, D.,
860 Russell, B.D., Santos, R., Serrano, O., Silliman, B.R., Watanabe, K., Duarte, C.M., 2019.
861 The future of Blue Carbon science. *Nat Commun* 10, 3998.
862 <https://doi.org/10.1038/s41467-019-11693-w>

863 Maes, J., Teller, A., Erhard, M., Condé, S., Vallecillo, S., Barredo, J.I., Luisa, M., Malak, D.A.,
864 Trombetti, M., Vigjak, O., Zulian, G., Addamo, A.M., Grizzetti, B., Somma, F., Hagyo, A.,
865 Vogt, P., Polce, C., Jones, A., Marin, A.I., Ivits, E., Mauri, A., Rega, C., Czúcz, B.,
866 Ceccherini, G., Pisoni, E., Ceglar, A., Palma, P. De, Cerrani, I., Meroni, M., Caudullo, G.,
867 Lugato, E., Vogt, J. V, Spinoni, J., Cammalleri, C., Bastrup-birk, A., Miguel, J.S., Román,
868 S.S., Kristensen, P., Christiansen, T., Roo, A. De, Cardoso, A.C., Pistocchi, A., Del, I.,
869 Alvarellós, B., Tsiamis, K., Gervasini, E., Deriu, I., Notte, A. La, Viñas, R.A., Vizzarri, M.,
870 Camia, A., Kakoulaki, G., Bendito, E.G., Panagos, P., Ballabio, C., Scarpa, S., Orgiazzi,
871 A., Ugalde, O.F., Santos-martín, F., 2020. Mapping and Assessment of Ecosystems and
872 their Services : An EU ecosystem assessment. <https://doi.org/10.2760/757183>

873 Maier, M., Weber, T.K.D., Fiedler, J., Fuß, R., Glatzel, S., Huth, V., Jordan, S., Jurasinski, G.,
874 Kutzbach, L., Schäfer, K., Weymann, D., Hagemann, U., 2022. Introduction of a
875 guideline for measurements of greenhouse gas fluxes from soils using non-steady-
876 state chambers. *Journal of Plant Nutrition and Soil Science* 185, 447–461.
877 <https://doi.org/10.1002/JPLN.202200199>

878 McGillicuddy, M., Warton, D.I., Popovic, G., Bolker, B.M., 2025. Parsimoniously Fitting Large
879 Multivariate Random Effects in glmmTMB. *J Stat Softw* 112, 1–19.
880 <https://doi.org/10.18637/jss.v112.i01>

881 Meli, P., Benayas, J.M.R., Balvanera, P., Ramos, M.M., 2014. Restoration Enhances Wetland
882 Biodiversity and Ecosystem Service Supply, but Results Are Context-Dependent: A
883 Meta-Analysis. *PLoS One* 9, e93507.
884 <https://doi.org/10.1371/JOURNAL.PONE.0093507>

885 Minaudo, C., Cabrera-Brufau, M., Montes-Pérez, J.J., Attermeyer, K., Camacho, A.,
886 Camacho-Santamans, A., Cazacu, C., Giuca, R., Lillebø, A., Misteli, B., Morant, D.,
887 Obrador, B., Oliveira, B., Petkuvienė, J., Picazo, A., Rochera, C., von Schiller, D., 2025.
888 Uncertainty in aquatic greenhouse gas flux estimates arises from subjective
889 processing of floating chamber time series. *EarthArXiv preprint*.
890 <https://doi.org/10.31223/X5MN29>

891 Minaudo, C., von Schiller, D., Misteli, B., Morant, D., Adamescu, M., Attermeyer, K., Basset,
892 A., Carballeira, R., Cazacu, C., Coelho, J.P., Guelmami, A., Hilaire, S., Miralles, J.,
893 Obrador, B., Petkuvienė, J., Picazo, A., Rochera, C., Santinelli, C., Teixeira, H., Titocci,
894 J., Vaicute, D., Camacho, A., 2023. Methodological manual. Deliverable D4.2 Horizon
895 RESTORE4Cs Project GA ID: 101056782.

896 Miralles-Lorenzo, J., Picazo, A., Rochera, C., Morant, D., Casamayor, E.O., Menéndez-Serra,
897 M., Camacho, A., 2025. Environmental Gradients and Conservation Status Determine
898 the Structure and Carbon-Related Metabolic Potential of the Prokaryotic Communities
899 of Mediterranean Inland Saline Shallow Lakes. *Ecol Evol* 15, e71286.
900 <https://doi.org/10.1002/ece3.71286>

901 Misteli, B., Morant, D., Camacho, A., Adamo, M., Bachi, G., Bègue, N., Bučas, M., Cabrera-
902 Brufau, M., Carballeira, R., Cavalcante, L., Cazacu, C., Coelho, J., Doebke, C., Dinu, V.,
903 Guelmami, A., Giuca, R., Kataržytė, M., Lillebø, A., Marin, A., Marangi, C., Minaudo, C.,
904 Montes-Pérez, J., Obrador, B., Oliveira, B., Petkuvienė, J., Picazo, A., van Puijenbroek,
905 M., Ronse, M., Rochera, C., Sánchez, A., Santinelli, C., Sousa, A., von Schiller, D.,
906 Attermeyer, K., Tropea, C., Vaičiūtė, D., 2025. Coastal Wetland Restoration and
907 Greenhouse Gas Pathways: A Global Meta-Analysis. *EarthArXiv preprint*.
908 <https://doi.org/10.31223/X51B39>

909 Mitsch, W.J., Bernal, B., Nahlik, A.M., Mander, Ü., Zhang, L., Anderson, C.J., Jørgensen, S.E.,
910 Brix, H., 2012. Wetlands, carbon, and climate change. *Landscape Ecology* 2012 28:4
911 28, 583–597. <https://doi.org/10.1007/S10980-012-9758-8>

912 Morant, D., Picazo, A., Rochera, C., Santamans, A.C., Miralles-Lorenzo, J., Camacho, A.,
913 2020a. Influence of the conservation status on carbon balances of semiarid coastal
914 Mediterranean wetlands. *Inland Waters* 10, 453–467.
915 <https://doi.org/10.1080/20442041.2020.1772033>

916 Morant, D., Picazo, A., Rochera, C., Santamans, A.C., Miralles-Lorenzo, J., Camacho-
917 Santamans, A., Ibañez, C., Martínez-Eixarch, M., Camacho, A., 2020b. Carbon
918 metabolic rates and GHG emissions in different wetland types of the Ebro Delta. *PLoS*
919 *One* 15, e0231713. <https://doi.org/10.1371/journal.pone.0231713>

920 Morant, D., Rochera, C., Picazo, A., Miralles-Lorenzo, J., Camacho-Santamans, A.,
921 Camacho, A., 2024. Ecological status and type of alteration determine the C-balance
922 and climate change mitigation capacity of Mediterranean inland saline shallow lakes.
923 *Sci Rep* 14, 29065. <https://doi.org/10.1038/s41598-024-79578-7>

924 Moreno-Mateos, D., Barbier, E.B., Jones, P.C., Jones, H.P., Aronson, J., López-López, J.A.,
925 McCrackin, M.L., Meli, P., Montoya, D., Rey Benayas, J.M., 2017. Anthropogenic
926 ecosystem disturbance and the recovery debt. *Nature Communications* 2017 8:1 8,
927 14163-. <https://doi.org/10.1038/ncomms14163>

928 Moreno-Mateos, D., Power, M.E., Comín, F.A., Yockteng, R., 2012. Structural and Functional
929 Loss in Restored Wetland Ecosystems. *PLoS Biol* 10, e1001247.
930 <https://doi.org/10.1371/JOURNAL.PBIO.1001247>

931 Neubauer, S.C., 2021. Global Warming Potential Is Not an Ecosystem Property. *Ecosystems*
932 2021 24:8 24, 2079–2089. <https://doi.org/10.1007/S10021-021-00631-X>

933 O'Connor, J.J., Fest, B.J., Sievers, M., Swearer, S.E., 2020. Impacts of land management
934 practices on blue carbon stocks and greenhouse gas fluxes in coastal ecosystems—A
935 meta-analysis. *Glob Chang Biol* 26, 1354–1366. <https://doi.org/10.1111/gcb.14946>

936 Oliveira, R.B., Camacho, A., Guelmami, A., Schroder, C., Bègue, N., Bučas, M., Cazacu, C.,
937 Ciravegna, E., Coelho, J.P., Relu Giuca, C., Hilaire, S., Kataržytė, M., Morant, D., Picazo,
938 A., Polman, N., van Puijenbroek, M., Raoult, J., Rochera, C., Ronse, M., Sella, L., Sousa,
939 A.I., Racoviceanu, T., Rota, F.S., Vaičiūtė, D., Lillebø, A.I., n.d. (Submitted) European
940 coastal wetlands datasets and their use in decision-support tools for policy
941 restoration objectives. *Environmental Science and Policy* (Under review).

942 Palmer, M.A., Zedler, J.B., Falk, D.A., 2016. *Ecological Theory and Restoration Ecology.*
943 *Foundations of Restoration Ecology: Second Edition* 3–26.
944 https://doi.org/10.5822/978-1-61091-698-1_1

945 Peterson, R.A., 2021. Finding Optimal Normalizing Transformations via `bestNormalize`. *R J*
946 13, 310–329. <https://doi.org/10.32614/RJ-2021-041>

947 Pörtner, H.-O., Scholes, R.J., Agard, J., Archer, E., Arneth, A., Bai, X., Barnes, D., Burrows,
948 M., Chan, L., Cheung, W.L. (William), Diamond, S., Donatti, C., Duarte, C., Eisenhauer,
949 N., Foden, W., Gasalla, M.A., Handa, C., Hickler, T., Hoegh-Guldberg, O., Ichii, K.,
950 Jacob, U., Insarov, G., Kiessling, W., Leadley, P., Leemans, R., Levin, L., Lim, M.,
951 Maharaj, S., Managi, S., Marquet, P.A., McElwee, P., Midgley, G., Oberdorff, T., Obura,
952 D., Osman Elasha, B., Pandit, R., Pascual, U., Pires, A.P.F., Popp, A., Reyes-García, V.,
953 Sankaran, M., Settele, J., Shin, Y.-J., Sintayehu, D.W., Smith, P., Steiner, N., Strassburg,
954 B., Sukumar, R., Trisos, C., Val, A.L., Wu, J., Aldrian, E., Parmesan, C., Pichs-Madruga,
955 R., Roberts, D.C., Rogers, A.D., Díaz, S., Fischer, M., Hashimoto, S., Lavorel, S., Wu, N.,
956 Ngo, H., 2021. Scientific outcome of the IPBES-IPCC co-sponsored workshop on
957 biodiversity and climate change. <https://doi.org/10.5281/ZENODO.5101125>

958 R Core Team, 2025. R: A Language and Environment for Statistical Computing.

959 Ramsar Convention, 1971. Convention on Wetlands of International Importance especially
960 as Waterfowl Habitat. Ramsar.

961 Reddy, K.R., DeLaune, R.D., Inglett, P.W., 2022. Biogeochemistry of Wetlands : Science and
962 Applications. Biogeochemistry of Wetlands. <https://doi.org/10.1201/9780429155833>

963 Regnier, P., Resplandy, L., Najjar, R.G., Ciais, P., 2022. The land-to-ocean loops of the global
964 carbon cycle. *Nature* 2022 603:7901 603, 401–410. [https://doi.org/10.1038/s41586-](https://doi.org/10.1038/s41586-021-04339-9)
965 021-04339-9

966 Remeikaite-Nikiene, N., Lujanienė, G., Malejevas, V., Barisevičiūtė, R., Žilius, M., Garnaga-
967 Budre, G., Stankevičius, A., 2016. Distribution and sources of organic matter in
968 sediments of the south-eastern Baltic Sea. *Journal of Marine Systems* 157, 75–81.
969 <https://doi.org/10.1016/J.JMARSYS.2015.12.011>

970 Rheault, K., Christiansen, J.R., Larsen, K.S., 2024. goFlux: A user-friendly way to calculate
971 GHG fluxes yourself, regardless of user experience. *J Open Source Softw* 9, 6393.
972 <https://doi.org/10.21105/joss.06393>

973 Rissanen, A.J., Jilbert, T., Simojoki, A., Mangayil, R., Aalto, S.L., Khanongnuch, R., Peura, S.,
974 Jäntti, H., 2023. Organic matter lability modifies the vertical structure of methane-
975 related microbial communities in lake sediments. *Microbiol Spectr* 11.
976 <https://doi.org/10.1128/spectrum.01955-23>

977 Rochera, C., Picazo, A., Morant, D., Miralles-Lorenzo, J., Sánchez-Ortega, V., Camacho, A.,
978 2025a. Linking Carbon Fluxes to Flooding Gradients in Sediments of Mediterranean
979 Wetlands. *ACS ES&T Water* 5, 2882–2890.
980 <https://doi.org/10.1021/acsestwater.4c00940>

981 Rochera, C., Picazo, A., Morant, D., Miralles-Lorenzo, J., Sánchez-Ortega, V., Camacho, A.,
982 2025b. Linking Carbon Fluxes to Flooding Gradients in Sediments of Mediterranean
983 Wetlands. *ACS ES&T Water* 5, 2882–2890.
984 <https://doi.org/10.1021/ACSESTWATER.4C00940>

985 Romm, J., Lezak, S., Alshamsi, A., 2025. Are Carbon Offsets Fixable? *Annu Rev Environ*
986 *Resour* 50, 649–680. <https://doi.org/10.1146/annurev-environ-112823-064813>

987 Rosentreter, J.A., Al-Haj, A.N., Fulweiler, R.W., Williamson, P., 2021. Methane and Nitrous
988 Oxide Emissions Complicate Coastal Blue Carbon Assessments. *Global Biogeochem*
989 *Cycles* 35, e2020GB006858. <https://doi.org/10.1029/2020GB006858>

990 Saunois, M., Bousquet, P., Poulter, B., Peregon, A., Ciais, P., Canadell, J.G., Dlugokencky,
991 E.J., Etiope, G., Bastviken, D., Houweling, S., Janssens-Maenhout, G., Tubiello, F.N.,
992 Castaldi, S., Jackson, R.B., Alexe, M., Arora, V.K., Beerling, D.J., Bergamaschi, P., Blake,
993 D.R., Brailsford, G., Brovkin, V., Bruhwiler, L., Crevoisier, C., Crill, P., Covey, K., Curry,
994 C., Frankenberg, C., Gedney, N., Höglund-Isaksson, L., Ishizawa, M., Ito, A., Joos, F.,
995 Kim, H.S., Kleinen, T., Krummel, P., Lamarque, J.F., Langenfelds, R., Locatelli, R.,
996 Machida, T., Maksyutov, S., McDonald, K.C., Marshall, J., Melton, J.R., Morino, I., Naik,
997 V., O'Doherty, S., Parmentier, F.J.W., Patra, P.K., Peng, C., Peng, S., Peters, G.P., Pison,
998 I., Prigent, C., Prinn, R., Ramonet, M., Riley, W.J., Saito, M., Santini, M., Schroeder, R.,
999 Simpson, I.J., Spahni, R., Steele, P., Takizawa, A., Thornton, B.F., Tian, H., Tohjima, Y.,

1000 Viovy, N., Voulgarakis, A., Van Weele, M., Van Der Werf, G.R., Weiss, R., Wiedinmyer,
1001 C., Wilton, D.J., Wiltshire, A., Worthy, D., Wunch, D., Xu, X., Yoshida, Y., Zhang, B.,
1002 Zhang, Z., Zhu, Q., 2016. The global methane budget 2000-2012. *Earth Syst Sci Data* 8,
1003 697–751. <https://doi.org/10.5194/ESSD-8-697-2016>

1004 Schorn, S., Ahmerkamp, S., Bullock, E., Weber, M., Lott, C., Liebeke, M., Lavik, G., Kuypers,
1005 M.M.M., Graf, J.S., Milucka, J., 2022. Diverse methylophilic methanogenic archaea
1006 cause high methane emissions from seagrass meadows. *Proc Natl Acad Sci U S A* 119.
1007 <https://doi.org/10.1073/PNAS.2106628119/-/DCSUPPLEMENTAL>

1008 Schuster, L., Taillardat, P., Macreadie, P.I., Malerba, M.E., 2024. Freshwater wetland
1009 restoration and conservation are long-term natural climate solutions. *Science of The*
1010 *Total Environment* 922, 171218. <https://doi.org/10.1016/j.scitotenv.2024.171218>

1011 Singh, N.K., Gourevitch, J.D., Wemple, B.C., Watson, K.B., Rizzo, D.M., Polasky, S., Ricketts,
1012 T.H., 2019. Optimizing wetland restoration to improve water quality at a regional scale.
1013 *Environmental Research Letters* 14, 064006. [https://doi.org/10.1088/1748-](https://doi.org/10.1088/1748-9326/AB1827)
1014 [9326/AB1827](https://doi.org/10.1088/1748-9326/AB1827)

1015 Suding, K.N., Gross, K.L., Houseman, G.R., 2004. Alternative states and positive feedbacks
1016 in restoration ecology. *Trends Ecol Evol* 19, 46–53.
1017 <https://doi.org/10.1016/j.tree.2003.10.005>

1018 Taillardat, P., Thompson, B.S., Garneau, M., Trottier, K., Friess, D.A., 2020. Climate change
1019 mitigation potential of wetlands and the cost-effectiveness of their restoration.
1020 *Interface Focus* 10, 20190129. <https://doi.org/10.1098/rsfs.2019.0129>

1021 Thieurmél, B., Elmarhraoui, A., 2022. suncalc: Compute Sun Position, Sunlight Phases,
1022 Moon Position and Lunar Phase. <https://doi.org/10.32614/CRAN.package.suncalc>

1023 Vaičiūtė, D., Bučas, M., Bresciani, M., Dabulevičienė, T., Gintauskas, J., Mėžinė, J., Tiškus,
1024 E., Umgiesser, G., Morkūnas, J., De Santi, F., Bartoli, M., 2021. Hot moments and
1025 hotspots of cyanobacteria hyperblooms in the Curonian Lagoon (SE Baltic Sea)
1026 revealed via remote sensing-based retrospective analysis. *Science of The Total*
1027 *Environment* 769, 145053. <https://doi.org/10.1016/j.scitotenv.2021.145053>

1028 Ward, S.E., Bardgett, R.D., McNamara, N.P., Ostle, N.J., 2009. Plant functional group identity
1029 influences short-term peatland ecosystem carbon flux: evidence from a plant removal
1030 experiment. *Funct Ecol* 23, 454–462. [https://doi.org/10.1111/J.1365-](https://doi.org/10.1111/J.1365-2435.2008.01521.X)
1031 [2435.2008.01521.X](https://doi.org/10.1111/J.1365-2435.2008.01521.X)

1032 Wickham, H., 2016. *ggplot2: Elegant Graphics for Data Analysis*. Springer-Verlag New York.

1033 Wickham, H., Pedersen, T.L., Seidel, D., 2025. scales: Scale Functions for Visualization.
1034 <https://doi.org/10.32614/CRAN.package.scales>

1035 Wu, Y., Sun, J., Hu, B., Zhang, G., Rousseau, A.N., 2023. Wetland-based solutions against
1036 extreme flood and severe drought: Efficiency evaluation of risk mitigation. *Clim Risk*
1037 *Manag* 40, 100505. <https://doi.org/10.1016/J.CRM.2023.100505>

1038 Zilius, M., Bartoli, M., Bresciani, M., Katarzyte, M., Ruginis, T., Petkuvienė, J., Lubiene, I.,
1039 Giardino, C., Bukaveckas, P.A., de Wit, R., Razinkovas-Baziukas, A., 2013. Feedback
1040 Mechanisms Between Cyanobacterial Blooms, Transient Hypoxia, and Benthic

1041 Phosphorus Regeneration in Shallow Coastal Environments. *Estuaries and Coasts*
1042 2013 37:3 37, 680–694. <https://doi.org/10.1007/S12237-013-9717-X>

1043 Zorrilla-Miras, P., Palomo, I., Gómez-Baggethun, E., Martín-López, B., Lomas, P.L., Montes,
1044 C., 2014. Effects of land-use change on wetland ecosystem services: A case study in
1045 the Doñana marshes (SW Spain). *Landsc Urban Plan* 122, 160–174.
1046 <https://doi.org/10.1016/J.LANDURBPLAN.2013.09.013>

1047

1048

Supplementary materials

1. Detailed description of European case pilot wetlands

South-West Dutch Delta (DU)

Preserved sites consisted of Intertidal salt marshes showing natural hydrological and sedimentation processes, vegetated surfaces, and minimal disruption by coastal infrastructure. These sites maintained natural marsh integrity and ecological processes including tidal inundation patterns, natural sedimentation, pioneer zone species, and mid-upper marsh communities. The main alterations were the installation of stone breakwaters or wooden pales perpendicular to the marsh to reduce hydrodynamics and locally reduce erosion. These hard structures disrupted natural sedimentation processes and reflected wave energy, leading to accelerated lateral erosion and creek widening, prevention of natural landward marsh development and disappearance of pioneer-zone plant species. Restoration involved morphological reconstruction and recovery of natural hydrodynamics through managed realignment. In both cases, the displacement of the coastal defense line further inland facilitated recovery of natural hydrodynamics, tidal patterns, sedimentation processes, and vegetation establishment on previously reclaimed land.

Ria de Aveiro (RI)

Preserved sites exhibited healthy intertidal seagrass meadows with high coverage of *Zostera noltii*, stable sediment structure, and absence of significant anthropogenic pressures. The main alteration consisted of erosion and bioturbation from bait-digging activities and physical disturbance from trampling. Altered sites consist of bare, unvegetated intertidal areas where meadows have been lost or severely degraded. These areas exhibit high erosion, unstable sediments prone to resuspension and reduced biodiversity. Restoration actions consisted of re-vegetation: Active mosaic-pattern transplantation of *Z. noltii* have been formerly performed in zones where pressures are no longer relevant. Transplants were able to cover previously unvegetated areas and develop uniform, robust coverage throughout the restored sites within one year.

Camargue (CA)

Preserved sites were selected from mediterranean freshwater marshes and ponds that retained natural hydrological regimes and ecological features, without significant historical land use conversion or hydrological alterations. These sites maintained intact soil and seasonal flooding and drying patterns characteristic of Mediterranean freshwater wetlands, supporting native flora and fauna. This case pilot suffered mainly from hydrological, trophic, and land-use change impacts. The altered sites included former fishponds and areas that had been subjected to decades of artificial hydrological regimes, mainly favoring hunting activities. These sites experienced hydrological alterations driven by artificial irrigation and drainage systems, leading to long-term changes in water regimes. The natural seasonal hydrological variability was replaced by highly managed water regimes, with continuous flooding during dry seasons. Restoration activities involved soil, hydrology, vegetation and morphological reconstruction of former rice fields and pastures. Topographic reshaping, removal of drainage and irrigation infrastructure, soil and seed transfers allowed for the recovery of natural flooding and drying cycles, recolonization by native wetland vegetation and increasing presence of amphibians and waterbirds in the sites.

1092 *Valencian wetland Marjal dels Moros (VA)*

1093 The selected preserved sites were coastal brackish marshes with intact emergent swamp
1094 communities, natural hydrological connectivity, and limited structural and water quality
1095 degradation. These areas featured native plant communities adapted to brackish
1096 conditions (reeds, bulrush stands and halophytic shrubs) and natural hydrodynamics
1097 controlled by precipitation, evaporation and seawater intrusion via groundwater. This
1098 wetland suffers mostly from hydrological, trophic, and morphological alterations. The
1099 representative altered sites are subject to artificial water supply from irrigation and
1100 wastewater sources as well as morphological modification (land-use change and soil
1101 degradation). These pressures resulted in areas with reduced native vegetation and
1102 proliferation of invasive species, and degraded water quality with elevated nutrients and
1103 loss of characteristic brackish conditions due to desalinization. As restored sites, areas
1104 were selected where various actions were performed. Active restoration included soil
1105 reconstruction to improve substrate conditions, morphological reconstruction of natural
1106 topology and hydrological connectivity, and planting of native vegetation. Hydrological
1107 actions ensure diverse good-quality water sources to maintain aquatic refuges for fauna via
1108 flood regulation while maintaining characteristic brackish conditions. Mowing of helophytic
1109 vegetation is regularly implemented to maintain habitat heterogeneity.

1110 *Danube Delta (DA)*

1111 Preserved sites consisted of freshwater shallow lakes with native submerged (*Potamogeton*
1112 *spp.*, *Ceratophyllum spp.*) and floating vegetation (*Trapa natans* L., *Nymphaea alba* L.)
1113 surrounded by reed beds (*Phragmites australis* L.). These sites lacked major anthropogenic
1114 pressures, maintained their connectivity to the river network and are classified as having
1115 good ecological status according to the Water Framework Directive. The most relevant
1116 impacts of this pilot are hydrological and morphological alterations related to land-use
1117 change. Altered sites were former freshwater wetlands converted to dryland during the
1118 1980s. One site consisted of an agricultural field used to grow cereal. The other site was
1119 initially used for pasture for cattle but was flooded due to dike failure and was subsequently
1120 abandoned for this use. These areas suffered lack of native vegetation, soil alteration and
1121 high nutrient loads from fertilizers and manure, respectively. Restoration activities
1122 consisted of the morphological and hydrological reconstruction of wetland habitats from
1123 former pastures and degraded wetlands. Restoration of sites involved the recovery of
1124 natural hydrological regimes via their re-connection to the river network and flood
1125 management via pumping stations, as well as the removal of excess reed cover to create
1126 open water habitats.

1127 *Curonian Lagoon (CU)*

1128 Preserved sites consisted of littoral zones characterized by high coverage of submerged
1129 aquatic vegetation (*Chara contraria*, *Chara apsera*, *Chara globularis*, *Potamogeton*
1130 *perfoliatus*, *Stuckenia pectinata*), with sandy or mixed bottom substrates and emergent
1131 reeds (*P. Australis*). The relatively low nutrient loads and chlorophyll-a concentrations of
1132 these areas are characteristic of balanced trophic conditions in the Lagoon. The most
1133 relevant pressures within the system consist of eutrophication and organic matter
1134 enrichment. Altered trophic state is driven by high nutrient loads from agricultural runoff
1135 and insufficient wastewater treatment from the Neumas river. The altered sites selected
1136 were characterized by elevated nutrient levels and associated high chlorophyll-a
1137 concentrations with episodic cyanobacterial blooms. The accumulation of organic-rich

mud in the substrate promotes anoxic conditions and leads to a reduction in submerged aquatic vegetation. Restoration actions at the watershed level aimed at improving water quality and local-scale measures, such as reed harvesting to reduce excess nutrients and organic matter. Improvements of wastewater treatment infrastructure and reduced fertilizer use in the upstream Nemunas river basin led to reduced nutrient loads. In addition, hydrological changes such as increased brackish water intrusions due to the artificial deepening of the Klaipėda Strait channel (Stakėnienė et al., 2023) and decreased annual runoff from the Nemunas River (Idzelyte- et al., 2023) have likely reduced fine sediment inputs and muddy sediment accumulation. These changes have affected recovery of sandy sediment areas and promoted the expansion of submerged aquatic vegetation in restored sites.

2. Best-flux estimate selection

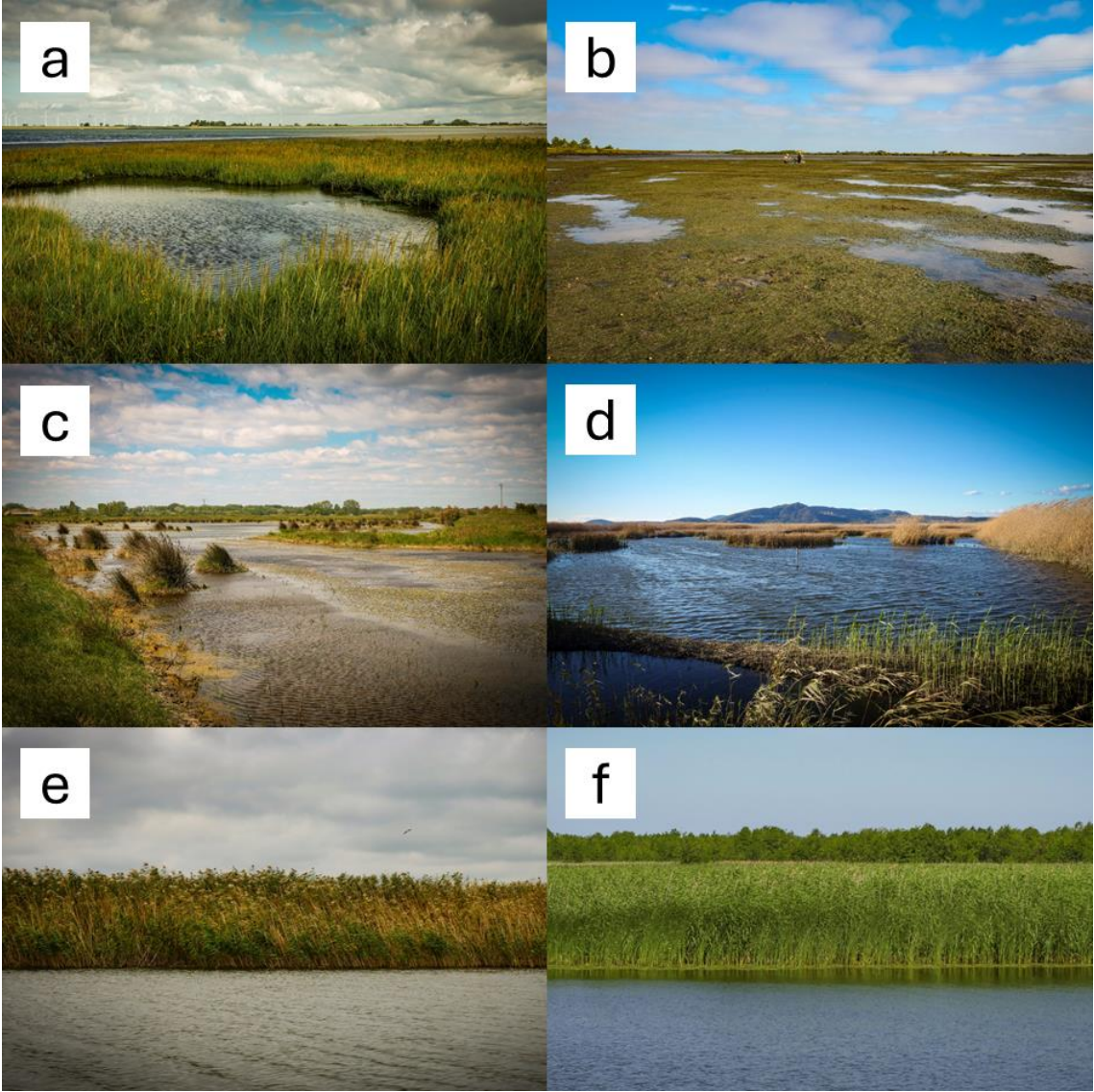
A common set of sequential criteria was followed to select a best-flux estimate from those produced by the three models: two-point, linear model (LM) and a non-linear (HM) (Hutchinson & Mosier, 1981) regression model. Choosing an appropriate flux calculation method is not trivial, as different approaches can result in large differences in estimated flux and have different sensitivities to non-linear patterns of gas concentration within the chamber, which may arise from both instrument noise and natural processes. On the one hand, simple linear regression (LM) often underestimates fluxes in non-steady chambers (Silva et al., 2015), which leads many researchers to default to non-linear (HM) model (Rheault et al., 2024). However, noisy measurements can lead to the HM model producing unrealistic fluxes (Hüppi et al., 2018). Additionally, ebullitive dynamics typically force extreme curvatures of HM and might even cause negative LM flux estimates. To select an appropriate best-estimate instantaneous flux for every time series, we used sequential criteria based on the presence of ebullitive patterns and on LM and HM model fit statistics. This set of criteria was designed to balance the model-specific risks of over- and underestimation of fluxes, especially for cases with ebullitive patterns, while preserving a transparent and reproduceable approach.

First, all CH₄ timeseries with visual evidence of ebullition (recorded during previous inspection) were assigned to the two-point flux estimate unless the linear model presented an R² above 0.99 (LM.r² > 0.99). For the rest of the timeseries, absent of ebullitive patterns, the HM model was chosen only when all the following criteria were met (defaulting to the LM estimate when one or more were violated): HM model produces a valid flux estimate (HM.flux ≠ NA); LM flux estimate is above the minimal detectable flux (Christiansen et al., 2015); HM curvature parameter *Kappa* is below the theoretical maximum (Hüppi et al., 2018); The ratio between the non-linear (HM) flux estimate and the linear (LM) estimate, the g-factor (Hüppi et al., 2018) is below the gas species-specific custom threshold (CO₂ g-factor < 4; CH₄ g-factor < 3); Akaike Information Criterion corrected for small sample size (AICc) of the HM model is lower than that of the LM model; Mean absolute error (MAE) of HM model is at least 5% lower than that of LM model.

A larger g-factor threshold was allowed for CO₂ time series (compared to CH₄) to account for cases where CO₂ concentration inside the chamber might cause limitation of photosynthetic activity and associated attenuation of uptake rate during the incubation. Using this set of criteria, the chosen best model for CO₂ fluxes was LM for 1914 timeseries

1182 (64%) and HM for 1076 timeseries (36%). For CH₄ fluxes, the best model was two-point for
1183 631 (21.1%), LM for 1850 (62%) and HM for 505 (16.9%) of the time series.

1184 3. Supplementary Figures



1185
1186 **Figure S1. Representative pictures of case pilot preserved wetlands.** Pictures
1187 depict (a) saltmarsh of South-west Dutch Delta (DU), (b) *Zostera noltii* meadow
1188 during low tide in Ria de Aveiro (RI), (c) freshwater marshes and ponds of Camargue
1189 (CA), (d) brackish marshes of Marjal dels Moros (VA), (e) freshwater lakes with reed
1190 beds of Danube Delta (DA), (f) freshwater littoral with reeds and submerged
1191 vegetation of Curonian Lagoon (CU). Pictures facilitated by LifeWatch ERIC.

1192

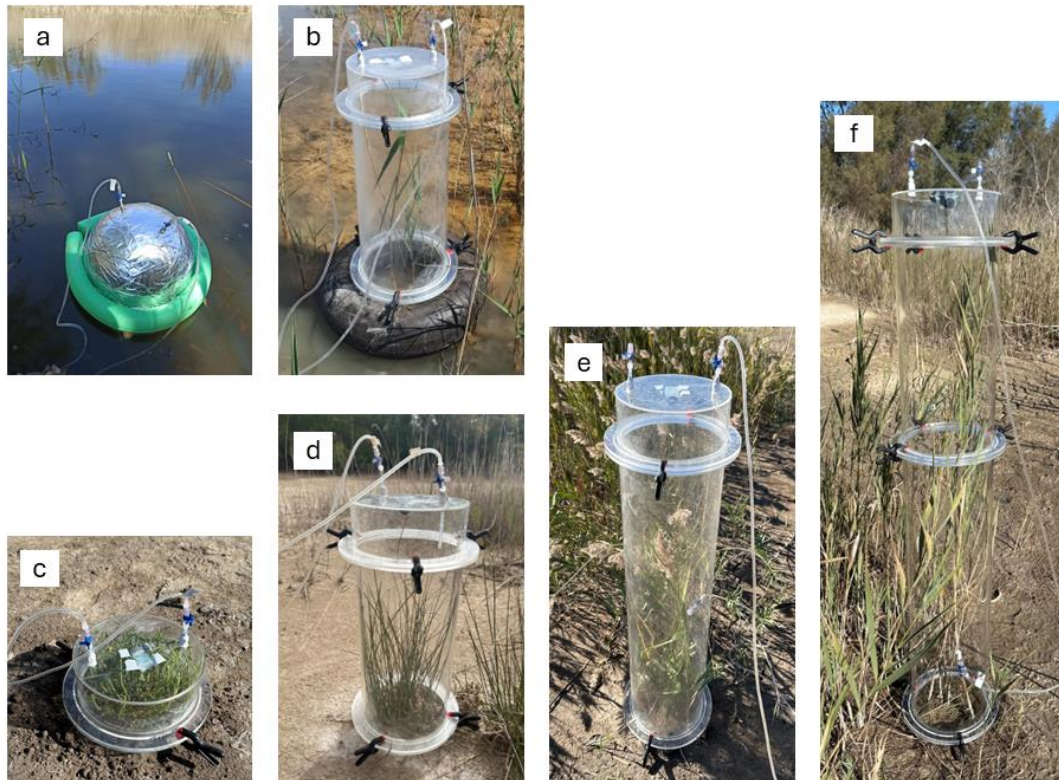


Figure S2. Static chamber types and configurations. (a) Opaque semi-spherical floating chamber used in open water areas, (b) transparent modular cylindrical chamber with floating device used in flooded areas with emergent vegetation, (c-f) transparent modular cylindrical chamber used in non-flooded areas in increasing-volume configurations. Dark incubations using the cylindrical modular chamber involved the use of an opaque textile cover (not shown).

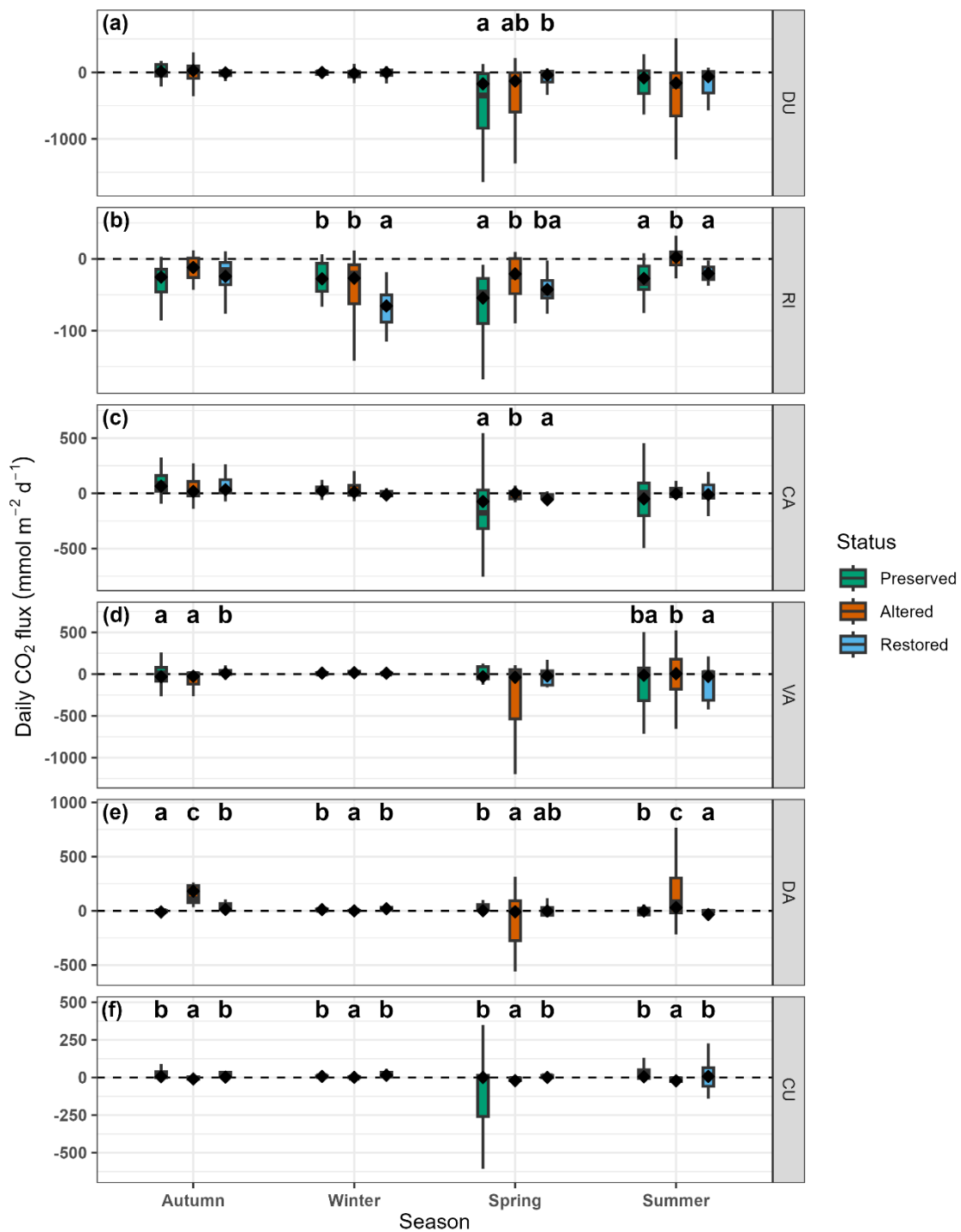


Figure S3. Daily CO₂ fluxes (mmol m⁻² d⁻¹) across seasons according to wetland conservation status for each case pilot (a-f panels). Boxplots show the median, interquartile range, and whiskers extending to 1.5xIQR; potential outliers (data outside the previously defined ranges) are not displayed for clarity. Diamonds represent GLMM-derived EMMs and letters represent significantly different EMM groups in each season ($p < 0.05$, post-hoc t- or z-test) alphabetically ordered according to group ranks.

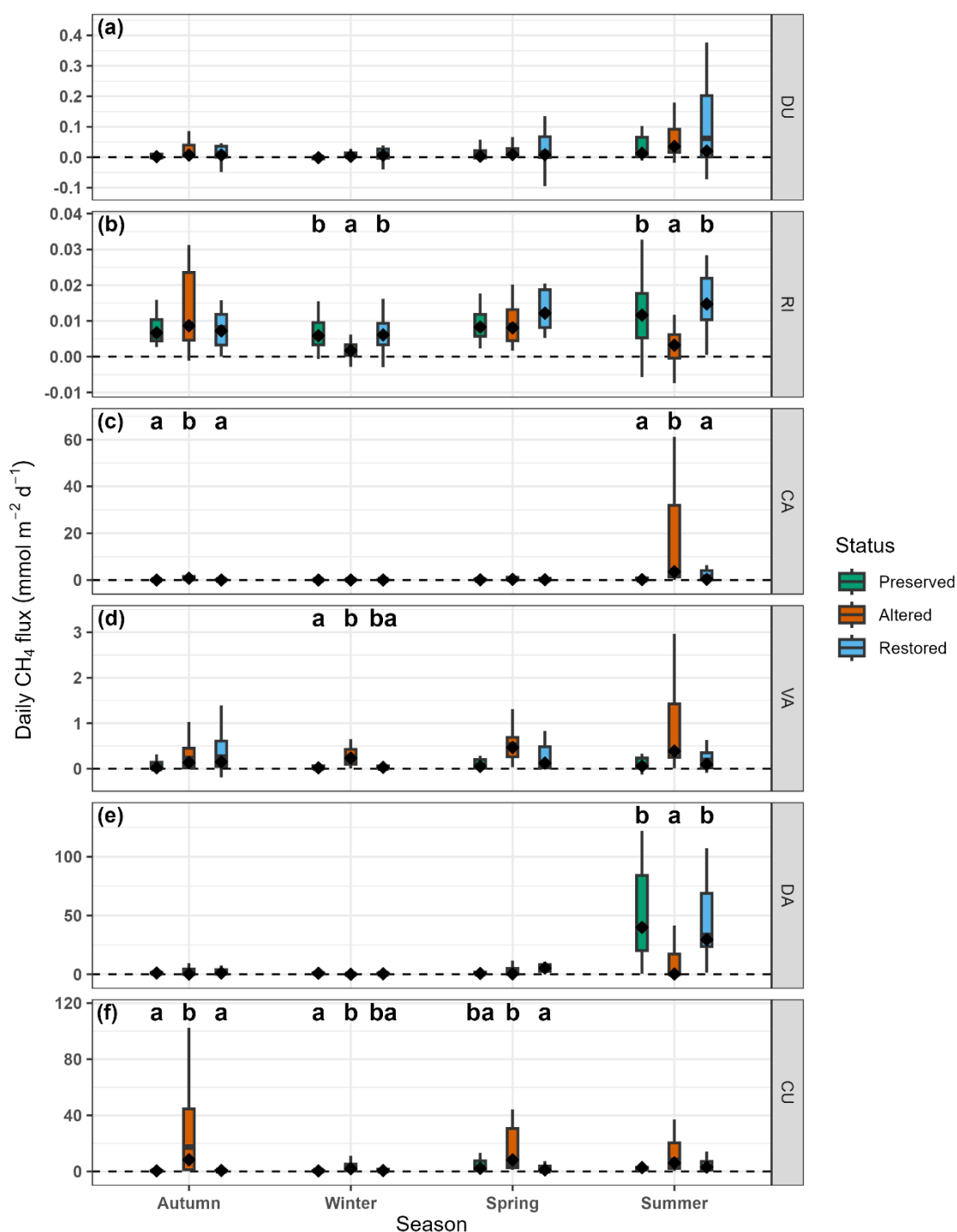


Figure S4. Daily CH₄ fluxes (mmol m⁻² d⁻¹) across seasons according to wetland conservation status for each case pilot (a-f panels). Boxplots show the median, interquartile range, and whiskers extending to 1.5xIQR; potential outliers (data outside the previously defined ranges) are not displayed for clarity. Diamonds represent GLMM-derived EMMs and letters represent significantly different EMM groups in each season (p < 0.05, post-hoc t- or z-test) alphabetically ordered according to group ranks.

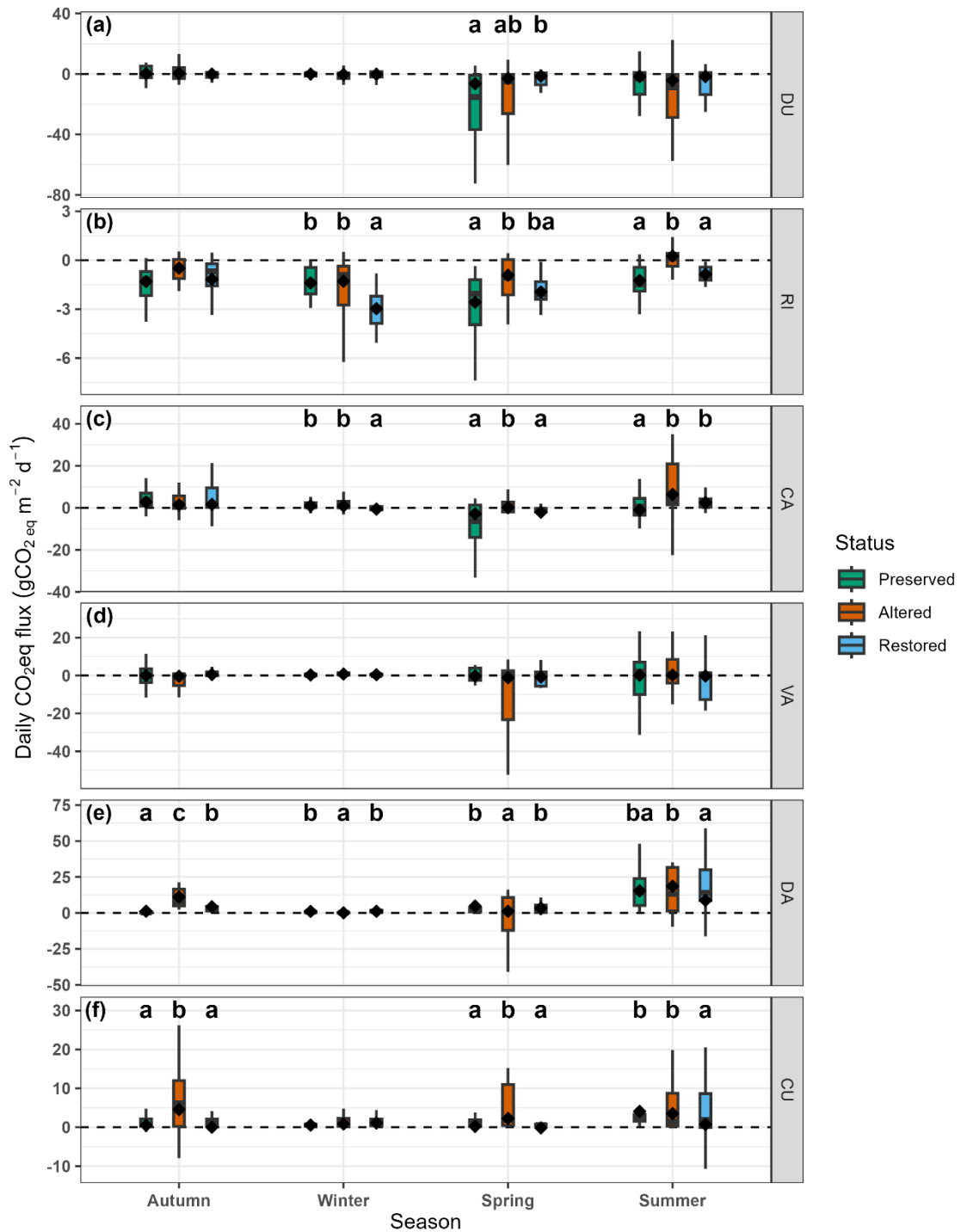


Figure S5. Daily CO₂-eq fluxes (g CO₂-eq m⁻² d⁻¹) across seasons according to wetland conservation status for each case pilot (a-f panels). Boxplots show the median, interquartile range, and whiskers extending to 1.5xIQR; potential outliers (data outside the previously defined ranges) are not displayed for clarity. Diamonds represent GLMM-derived EMMs and letters represent significantly different EMM groups in each season (p<0.05, post-hoc t- or z-test) alphabetically ordered according to group ranks.

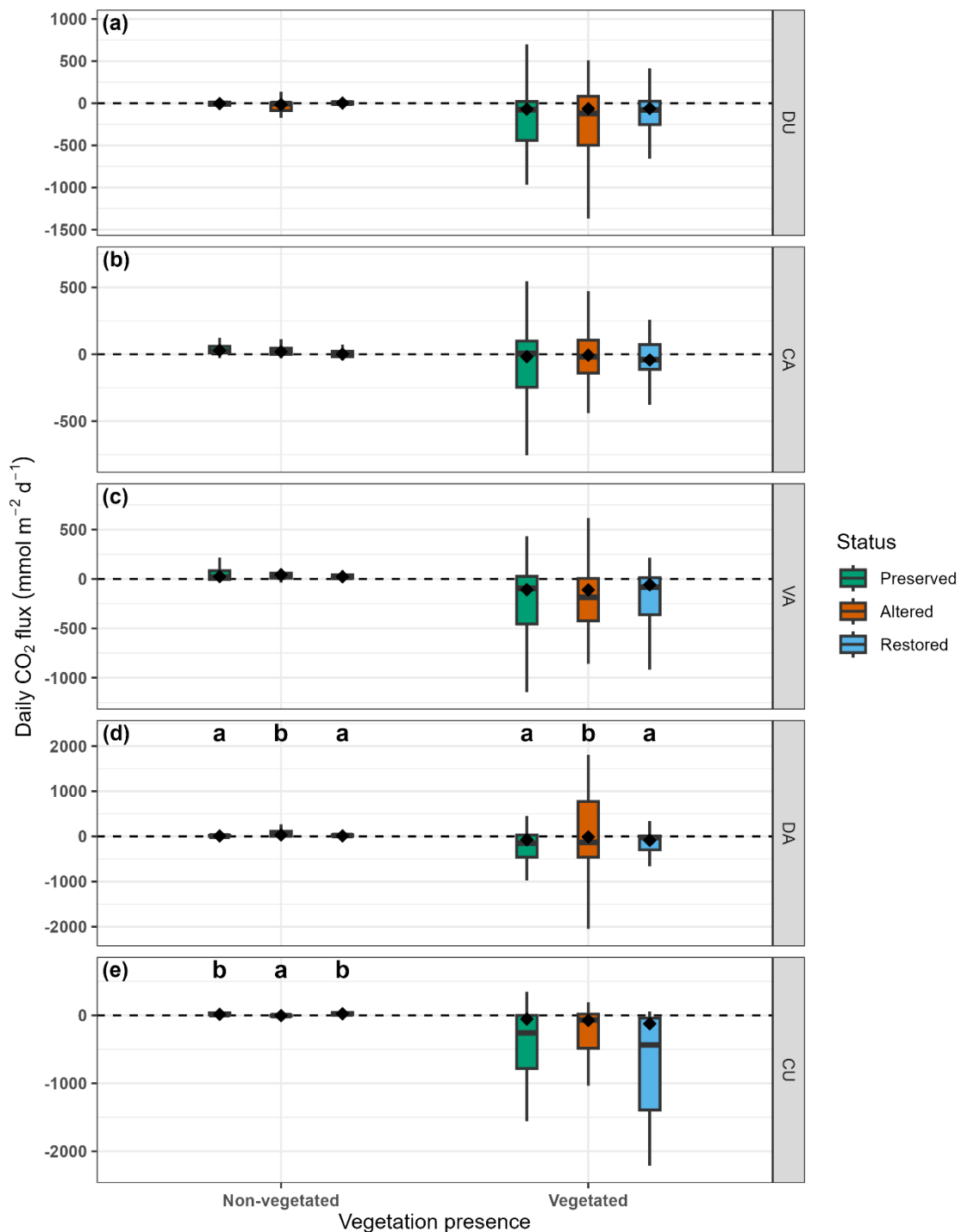


Figure S6. Daily CO₂ fluxes (mmol m⁻² d⁻¹) according to vegetation presence and wetland conservation status for each case pilot (a-f panels). Boxplots show the median, interquartile range, and whiskers extending to 1.5xIQR; potential outliers (data outside the previously defined ranges) are not displayed for clarity. Diamonds represent GLMM-derived EMMs and letters represent significantly different EMM groups in each season (p < 0.05, post-hoc t- or z-test) alphabetically ordered according to group ranks.

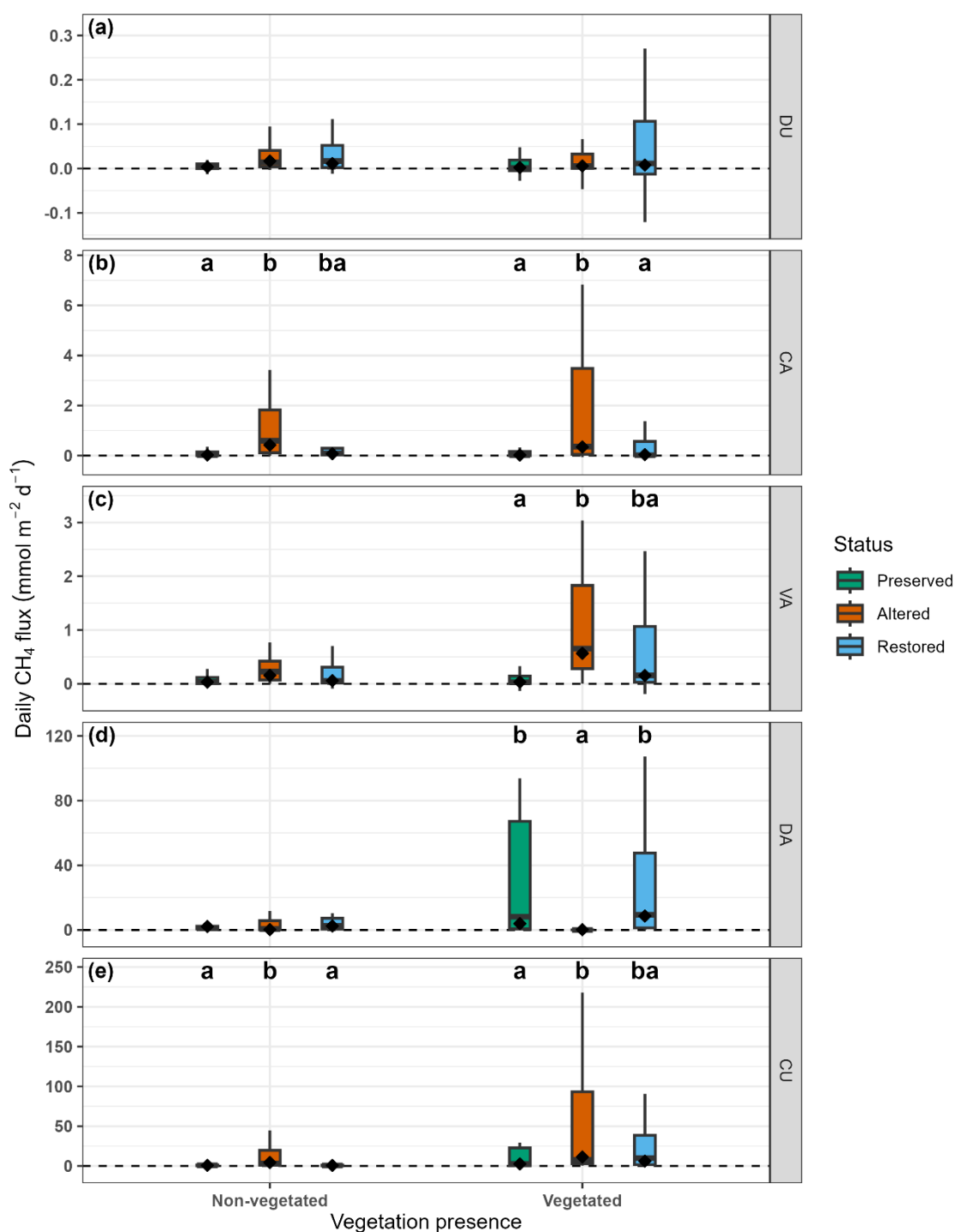


Figure S7. Daily CH₄ fluxes (mmol m⁻² d⁻¹) according to vegetation presence and wetland conservation status for each case pilot (a-f panels). Boxplots show the median, interquartile range, and whiskers extending to 1.5xIQR; potential outliers (data outside the previously defined ranges) are not displayed for clarity. Diamonds represent GLMM-derived EMMs and letters represent significantly different EMM groups in each season (p < 0.05, post-hoc t- or z-test) alphabetically ordered according to group ranks.

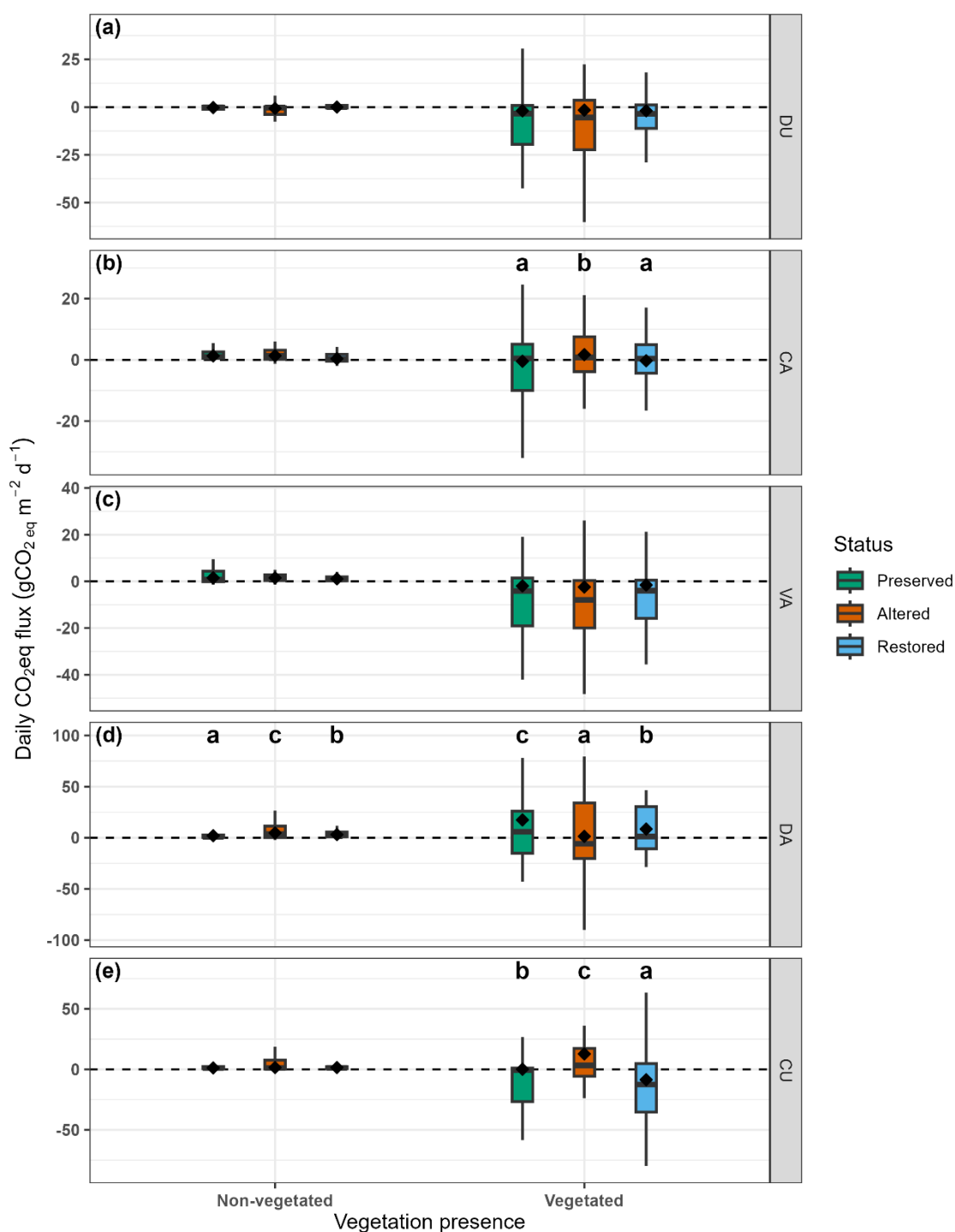


Figure S8. Daily CO₂-eq fluxes (g CO₂-eq m⁻² d⁻¹) according to vegetation presence and wetland conservation status for each case pilot (a-f panels). Boxplots show the median, interquartile range, and whiskers extending to 1.5xIQR; potential outliers (data outside the previously defined ranges) are not displayed for clarity. Diamonds represent GLMM-derived EMMs and letters represent significantly different EMM groups in each season (p < 0.05, post-hoc t- or z-test) alphabetically ordered according to group ranks.

4. Supplementary tables

Table S1. GLMM model summaries. Model structure (formula call, distribution and data transformation), number of samples (N), marginal and conditional R-squared values (R^2_m and R^2_c) representing the proportion of variance explained by the model and significance of fixed effects (conservation status, season, vegetation presence and interactions) for each case pilot-GHG flux dataset.

Dataset	Best-Supported Model	N	R^2_m	R^2_c	Effect	p-Value
DU - CO ₂	Call: Flux ~ status * season * vegpresence + (1 site), Distribution: t, Transformation: pseudo-log	349	0.494	0.515	status	0.764
					season	< 0.001
					vegpresence	< 0.001
					status : season	0.011
					status : vegpresence	0.418
					status : season : vegpresence	0.014
RI - CO ₂	Call: Flux ~ status * season + (1 site), Distribution: gaussian, Transformation: pseudo-log	266	0.315	0.347	status	< 0.001
					season	< 0.001
					status : season	0.001
CA - CO ₂	Call: Flux ~ status * season * vegpresence + (1 site), Distribution: t, Transformation: pseudo-log	346	0.473	0.537	status	0.268
					season	< 0.001
					vegpresence	< 0.001
					status : season	< 0.001
					status : vegpresence	0.206
					status : season : vegpresence	< 0.001

Dataset	Best-Supported Model	N	R ² m	R ² c	Effect	p-Value
VA - CO ₂	Call: Flux ~ status * season * vegpresence + (1 site), Distribution: t, Transformation: pseudo-log	340	0.741	0.749	status	0.627
					season	< 0.001
					vegpresence	< 0.001
					status : season	< 0.001
					status : vegpresence	0.001
					status : season : vegpresence	< 0.001
DA - CO ₂	Call: Flux ~ status * season * vegpresence + (1 site), Distribution: t, Transformation: pseudo-log	296	0.800	0.800	status	< 0.001
					season	< 0.001
					vegpresence	< 0.001
					status : season	< 0.001
					status : vegpresence	0.003
					status : season : vegpresence	< 0.001
CU - CO ₂	Call: Flux ~ status * season * vegpresence + (1 site), Distribution: t, Transformation: pseudo-log	320	0.763	0.764	status	< 0.001
					season	< 0.001
					vegpresence	< 0.001
					status : season	< 0.001
					status : vegpresence	< 0.001
					status : season : vegpresence	< 0.001
DU - CH ₄		346	0.141	0.285	status	0.521

Dataset	Best-Supported Model	N	R ² m	R ² c	Effect	p-Value
	Call: Flux ~ status * season * vegpresence + (1 site), Distribution: gaussian, Transformation: pseudo-log				season	< 0.001
					vegpresence	0.02
					status : season	0.715
					status : vegpresence	0.379
					status : season : vegpresence	0.945
RI - CH ₄	Call: Flux ~ status * season + (1 site), Distribution: t, Transformation: pseudo-log	265	0.221	0.225	status	< 0.001
					season	< 0.001
					status : season	< 0.001
CA - CH ₄	Call: Flux ~ status * season * vegpresence + (1 site), Distribution: gaussian, Transformation: pseudo-log	345	0.390	0.436	status	0.001
					season	< 0.001
					vegpresence	0.232
					status : season	< 0.001
					status : vegpresence	0.78
VA - CH ₄	Call: Flux ~ status * season * vegpresence + (1 site), Distribution: gaussian, Transformation: pseudo-log	337	0.262	0.393	status : season : vegpresence	0.491
					status	0.039
					season	0.005
					vegpresence	< 0.001
					status : season	0.057
					status : vegpresence	0.04

Dataset	Best-Supported Model	N	R ² m	R ² c	Effect	p-Value
DA - CH ₄	Call: Flux ~ status * season * vegpresence + (1 site), Distribution: t, Transformation: log	306	0.502	0.678	status : season : vegpresence	0.63
					status	0.011
					season	< 0.001
					vegpresence	0.026
					status : season	< 0.001
					status : vegpresence	0.046
					status : season : vegpresence	< 0.001
CU - CH ₄	Call: Flux ~ status * season * vegpresence + (1 site), Distribution: gaussian, Transformation: pseudo-log	317	0.526	0.585	status	0.003
					season	< 0.001
					vegpresence	< 0.001
					status : season	< 0.001
					status : vegpresence	0.012
					status : season : vegpresence	0.005
DU - CO ₂ -eq	Call: Flux ~ status * season * vegpresence + (1 site), Distribution: gaussian, Transformation: arcsinh	345	0.382	0.393	status	0.757
					season	< 0.001
					vegpresence	< 0.001
					status : season	0.211
					status : vegpresence	0.192
					status : season : vegpresence	0.252

Dataset	Best-Supported Model	N	R ² m	R ² c	Effect	p-Value
RI - CO ₂ -eq	Call: Flux ~ status * season + (1 site), Distribution: gaussian, Transformation: Yeo-Johnson	263	0.325	0.343	status	< 0.001
					season	< 0.001
					status : season	0.003
CA - CO ₂ -eq	Call: Flux ~ status * season * vegpresence + (1 site), Distribution: t, Transformation: arcsinh	342	0.489	0.514	status	0.026
					season	< 0.001
					vegpresence	< 0.001
					status : season	< 0.001
					status : vegpresence	0.004
					status : season : vegpresence	< 0.001
VA - CO ₂ -eq	Call: Flux ~ status * season * vegpresence + (1 site), Distribution: gaussian, Transformation: arcsinh	333	0.527	0.545	status	0.96
					season	< 0.001
					vegpresence	< 0.001
					status : season	0.368
					status : vegpresence	0.304
					status : season : vegpresence	0.148
DA - CO ₂ -eq	Call: Flux ~ status * season * vegpresence + (1 site), Distribution: t, Transformation: arcsinh	292	0.718	0.718	status	< 0.001
					season	< 0.001
					vegpresence	< 0.001
					status : season	< 0.001

Dataset	Best-Supported Model	N	R ² m	R ² c	Effect	p-Value
CU - CO ₂ -eq	Call: Flux ~ status * season * vegpresence + (1 site), Distribution: t, Transformation: pseudo-log	312	0.656	0.682	status : vegpresence	< 0.001
					status : season : vegpresence	< 0.001
					status	< 0.001
					season	< 0.001
					vegpresence	< 0.001
					status : season	< 0.001
					status : vegpresence	< 0.001
					status : season : vegpresence	< 0.001

Table S2. Model-derived estimated marginal means (EMMs). EMM, standard error and 95% confidence interval of GHG fluxes (CO₂, CH₄, CO₂-eq) for different conservation status of each case pilot wetland across seasons and vegetation presence.

Case pilot	Status	CO ₂ flux (mmol m ⁻² d ⁻¹)		CH ₄ flux (mmol m ⁻² d ⁻¹)		GWP flux (g CO ₂ -eq. m ⁻² d ⁻¹)	
		Mean ± SE	95% CI	Mean ± SE	95% CI	Mean ± SE	95% CI
RI	Preserved	-32.4 ± 5.14	-42.6 to -22.3	0.0079 ± 0.00075	0.00643 to 0.00937	-1.59 ± 0.228	-2.04 to -1.14
	Altered	-13.4 ± 3.44	-20.2 to -6.64	0.00492 ± 0.000564	0.00381 to 0.00602	-0.519 ± 0.148	-0.812 to -0.227
	Restored	-35.4 ± 5.68	-46.6 to -24.2	0.00953 ± 0.000916	0.00773 to 0.0113	-1.65 ± 0.245	-2.13 to -1.17
DU	Preserved	-37.8 ± 13.8	-64.8 to -10.7	0.00272 ± 0.00315	-0.00347 to 0.00892	-1.09 ± 0.346	-1.77 to -0.405
	Altered	-42.1 ± 13.6	-68.8 to -15.4	0.00921 ± 0.00698	-0.00453 to 0.0229	-1.18 ± 0.36	-1.88 to -0.466
	Restored	-26.1 ± 11	-47.7 to -4.63	0.00921 ± 0.00701	-0.00458 to 0.023	-0.765 ± 0.301	-1.36 to -0.172
CA	Preserved	-5.13 ± 10.5	-25.7 to 15.4	0.0237 ± 0.0134	-0.00259 to 0.0501	-0.00711 ± 0.289	-0.574 to 0.56
	Altered	6.1 ± 10.7	-14.9 to 27.1	0.384 ± 0.215	-0.038 to 0.806	1.5 ± 0.58	0.364 to 2.64
	Restored	-9.67 ± 11.2	-31.6 to 12.3	0.0583 ± 0.0328	-0.00627 to 0.123	0.227 ± 0.3	-0.361 to 0.816
VA	Preserved	-13.8 ± 5.95	-25.4 to -2.13	0.0312 ± 0.0197	-0.00763 to 0.07	0.0204 ± 0.254	-0.48 to 0.521
	Altered	-7.98 ± 4.46	-16.7 to 0.755	0.273 ± 0.169	-0.0592 to 0.606	-0.133 ± 0.258	-0.64 to 0.374
	Restored	-6.3 ± 5.02	-16.1 to 3.55	0.0839 ± 0.0521	-0.0186 to 0.186	-0.0359 ± 0.258	-0.543 to 0.471
DA	Preserved	-0.0447 ± 0.844	-1.7 to 1.61	2.38 ± 1.85	-1.25 to 6	3.3 ± 0.241	2.83 to 3.77
	Altered	13.9 ± 1.4	11.2 to 16.6	0.182 ± 0.17	-0.151 to 0.514	3.4 ± 0.267	2.87 to 3.92
	Restored	1.07 ± 1.11	-1.1 to 3.24	3.07 ± 2.4	-1.63 to 7.77	3.56 ± 0.352	2.87 to 4.25
CU	Preserved	4.13 ± 0.801	2.56 to 5.7	0.982 ± 0.339	0.316 to 1.65	0.89 ± 0.293	0.316 to 1.46
	Altered	-8.7 ± 1.36	-11.4 to -6.04	5.32 ± 1.83	1.72 to 8.92	2.41 ± 0.657	1.12 to 3.7
	Restored	5 ± 0.895	3.24 to 6.75	1.07 ± 0.374	0.337 to 1.81	0.346 ± 0.226	-0.098 to 0.789

Table S3. Post-hoc contrasts between model-derived averages (EMMs) of (a) CO₂, (b) CH₄ and (c) CO₂-eq daily fluxes between different conservation status classes of each case pilot. Estimate, standard error, 95% confidence interval and significance (P-value) are provided for each conservation status contrast across seasons. Negative flux differences for Preserved – Altered contrast represent avoided emissions through conservation. Negative flux differences for Restored – Altered contrasts represent mitigated emissions through restoration. Positive flux differences for Restored – Preserved contrasts represent functional recovery debt of restoration. All significance tests were computed in model-scale using t-tests or z-tests (for gaussian or t-family models, respectively) and flux differences were back-transformed according to the dataset-specific transformation function (Table S1).

Table S3a. Daily CO₂ flux contrasts for conservation status across seasons.

Case pilot	Contrast	Daily CO ₂ flux difference (mmol m ⁻² d ⁻¹)		
		Estimate ± SE	95% CI	P-value
DU	Preserved - Altered	4.33 ± 19.4	-33.6 to 42.3	0.994
	Restored - Altered	15.9 ± 17.5	-18.3 to 50.2	0.73
	Restored - Preserved	11.6 ± 17.6	-22.9 to 46.2	0.878
RI	Preserved - Altered	-19 ± 6.19	-31.2 to -6.84	0.004
	Restored - Altered	-22 ± 6.64	-35.1 to -8.93	0.001
	Restored - Preserved	-2.99 ± 7.66	-18.1 to 12.1	0.972
CA	Preserved - Altered	-11.2 ± 15	-40.6 to 18.2	0.831
	Restored - Altered	-15.8 ± 15.5	-46.2 to 14.6	0.65
	Restored - Preserved	-4.54 ± 15.3	-34.6 to 25.5	0.987
VA	Preserved - Altered	-5.81 ± 7.43	-20.4 to 8.75	0.817
	Restored - Altered	1.68 ± 6.71	-11.5 to 14.8	0.992
	Restored - Preserved	7.49 ± 7.78	-7.76 to 22.7	0.703
DA	Preserved - Altered	-13.9 ± 1.63	-17.1 to -10.7	< 0.001
	Restored - Altered	-12.8 ± 1.78	-16.3 to -9.33	< 0.001
	Restored - Preserved	1.11 ± 1.39	-1.61 to 3.84	0.81
CU	Preserved - Altered	12.8 ± 1.58	9.74 to 15.9	< 0.001
	Restored - Altered	13.7 ± 1.63	10.5 to 16.9	< 0.001
	Restored - Preserved	0.862 ± 1.2	-1.49 to 3.22	0.852

Table S3b. Daily CH₄ flux contrasts for conservation status across seasons.

Case pilot	Contrast	Daily CH ₄ flux difference (mmol m ⁻² d ⁻¹)		
		Estimate ± SE	95% CI	P-value
DU	Preserved - Altered	-0.00648 ± 0.00766	-0.0215 to 0.00858	0.699
	Restored - Altered	4.6e-06 ± 0.00989	-0.0195 to 0.0195	1
	Restored - Preserved	0.00649 ± 0.00768	-0.00863 to 0.0216	0.7
RI	Preserved - Altered	0.00299 ± 0.000938	0.00115 to 0.00482	0.004
	Restored - Altered	0.00461 ± 0.00108	0.0025 to 0.00672	< 0.001
	Restored - Preserved	0.00163 ± 0.00118	-0.000694 to 0.00395	0.42
CA	Preserved - Altered	-0.36 ± 0.215	-0.783 to 0.0626	0.002
	Restored - Altered	-0.326 ± 0.217	-0.753 to 0.101	0.053
	Restored - Preserved	0.0345 ± 0.0354	-0.0352 to 0.104	0.596
VA	Preserved - Altered	-0.242 ± 0.17	-0.577 to 0.0926	0.041
	Restored - Altered	-0.19 ± 0.177	-0.538 to 0.159	0.445
	Restored - Preserved	0.0527 ± 0.0557	-0.0569 to 0.162	0.601
DA	Preserved - Altered	2.2 ± 1.86	-1.44 to 5.83	0.08
	Restored - Altered	2.89 ± 2.4	-1.82 to 7.6	0.044
	Restored - Preserved	0.691 ± 3.03	-5.24 to 6.62	0.994
CU	Preserved - Altered	-4.34 ± 1.86	-8 to -0.68	0.002
	Restored - Altered	-4.25 ± 1.87	-7.93 to -0.577	0.004
	Restored - Preserved	0.09 ± 0.504	-0.902 to 1.08	0.997

Table S3b. Daily CO₂-eq flux contrasts for conservation status across seasons.

Case pilot	Contrast	Daily CO ₂ -eq difference (g CO ₂ -eq m ⁻² d ⁻¹)		
		Estimate ± SE	95% CI	P-value
DU	Preserved - Altered	0.0889 ± 0.5	-0.895 to 1.07	0.997
	Restored - Altered	0.41 ± 0.47	-0.515 to 1.33	0.761
	Restored - Preserved	0.321 ± 0.459	-0.582 to 1.22	0.861
RI	Preserved - Altered	-1.07 ± 0.272	-1.61 to -0.538	< 0.001

Case pilot	Contrast	Daily CO ₂ -eq difference (g CO ₂ -eq m ⁻² d ⁻¹)		
		Estimate ± SE	95% CI	P-value
	Restored - Altered	-1.13 ± 0.286	-1.69 to -0.566	< 0.001
	Restored - Preserved	-0.0568 ± 0.334	-0.715 to 0.601	0.998
	Preserved - Altered	-1.51 ± 0.648	-2.78 to -0.238	0.018
CA	Restored - Altered	-1.27 ± 0.653	-2.55 to 0.00645	0.085
	Restored - Preserved	0.234 ± 0.417	-0.583 to 1.05	0.92
	Preserved - Altered	0.153 ± 0.362	-0.559 to 0.866	0.965
VA	Restored - Altered	0.0969 ± 0.364	-0.62 to 0.814	0.991
	Restored - Preserved	-0.0564 ± 0.362	-0.769 to 0.656	0.998
	Preserved - Altered	-0.0967 ± 0.36	-0.802 to 0.608	0.99
DA	Restored - Altered	0.161 ± 0.442	-0.705 to 1.03	0.977
	Restored - Preserved	0.258 ± 0.427	-0.578 to 1.09	0.905
	Preserved - Altered	-1.52 ± 0.719	-2.93 to -0.11	0.046
CU	Restored - Altered	-2.06 ± 0.695	-3.43 to -0.702	< 0.001
	Restored - Preserved	-0.544 ± 0.37	-1.27 to 0.181	0.344
	Preserved - Altered			

Table S4. Summary of surface water parameters for different conservation status of each case pilot wetland. Chlorophyll-a (Chl-a), electrical conductivity (EC), total nitrogen (Total N) and total phosphorus (Total P) were determined using common analytical techniques (Santinelli et al., submitted). Total nitrogen and phosphorus include both particulate and dissolved nutrients.

Case pilot	Status	N	Chl-a ($\mu\text{g L}^{-1}$)	EC (mS cm^{-1})	Total N (μM)	Total P (μM)
			Mean \pm SE	Mean \pm SE	Mean \pm SE	Mean \pm SE
DU	Preserved	24	4.40 \pm 0.77	22.73 \pm 2.57	90.98 \pm 13.39	3.85 \pm 0.49
	Altered	24	7.17 \pm 2.87	24.75 \pm 2.40	92.29 \pm 15.65	13.01 \pm 4.51
	Restored	24	3.66 \pm 0.72	23.47 \pm 2.64	107.24 \pm 14.28	5.53 \pm 0.84
RI	Preserved	24	1.66 \pm 0.25	32.76 \pm 2.60	40.76 \pm 4.65	1.38 \pm 0.06
	Altered	24	1.76 \pm 0.21	26.16 \pm 2.90	75.40 \pm 9.28	1.62 \pm 0.06
	Restored	24	3.18 \pm 0.51	25.28 \pm 3.31	113.47 \pm 19.88	1.77 \pm 0.13
CA	Preserved	21	27.56 \pm 12.64	9.80 \pm 1.17	258.42 \pm 20.85	9.02 \pm 1.73
	Altered	21	10.41 \pm 2.41	3.50 \pm 0.68	147.15 \pm 19.56	6.23 \pm 1.50
	Restored	24	2.21 \pm 0.50	1.19 \pm 0.10	73.49 \pm 9.12	1.49 \pm 0.23
VA	Preserved	16	20.77 \pm 3.56	84.07 \pm 13.21	1513.66 \pm 461.66	14.32 \pm 9.22
	Altered	24	13.95 \pm 3.97	17.67 \pm 1.26	286.56 \pm 32.97	1.09 \pm 0.13
	Restored	21	35.35 \pm 9.53	60.16 \pm 6.37	703.78 \pm 80.30	4.90 \pm 0.66
DA	Preserved	24	49.23 \pm 10.56	0.52 \pm 0.03	137.98 \pm 28.56	1.74 \pm 0.27
	Altered	12	131.64 \pm 45.96	0.66 \pm 0.09	290.10 \pm 98.31	15.67 \pm 4.59
	Restored	24	28.11 \pm 6.96	1.40 \pm 0.25	237.76 \pm 27.71	3.00 \pm 0.61
CU	Preserved	24	8.17 \pm 1.30	0.53 \pm 0.11	124.06 \pm 13.90	2.88 \pm 0.61
	Altered	24	64.15 \pm 7.88	0.32 \pm 0.01	217.69 \pm 22.22	5.85 \pm 0.76
	Restored	24	27.50 \pm 4.82	0.32 \pm 0.01	137.27 \pm 16.38	2.32 0.27

5. Supplementary references

- Christiansen, J. R., Outhwaite, J., & Smukler, S. M. (2015). Comparison of CO₂, CH₄ and N₂O soil-atmosphere exchange measured in static chambers with cavity ring-down spectroscopy and gas chromatography. *Agricultural and Forest Meteorology*, 211–212, 48–57. <https://doi.org/10.1016/J.AGRFORMET.2015.06.004>
- Hüppi, R., Felber, R., Krauss, M., Six, J., Leifeld, J., & Fuß, R. (2018). Restricting the nonlinearity parameter in soil greenhouse gas flux calculation for more reliable flux estimates. *PLOS ONE*, 13(7), e0200876. <https://doi.org/10.1371/journal.pone.0200876>
- Hutchinson, G. L., & Mosier, A. R. (1981). Improved Soil Cover Method for Field Measurement of Nitrous Oxide Fluxes. *Soil Science Society of America Journal*, 45(2), 311–316. <https://doi.org/10.2136/sssaj1981.03615995004500020017x>
- Idzelyte-, R., Cerkasova, N., Mezine-, J., Dabulevičiene-, T., Razinkovas-Baziukas, A., Ertürk, A., & Umgiesser, G. (2023). Coupled hydrological and hydrodynamic modelling application for climate change impact assessment in the Nemunas river watershed-Curonian Lagoon-southeastern Baltic Sea continuum. *Ocean Science*, 19(4), 1047–1066. <https://doi.org/10.5194/OS-19-1047-2023>
- Rheault, K., Christiansen, J. R., & Larsen, K. S. (2024). goFlux: A user-friendly way to calculate GHG fluxes yourself, regardless of user experience. *Journal of Open Source Software*, 9(96), 6393. <https://doi.org/10.21105/joss.06393>
- Santinelli, C., Rochera, C., Tropea, C., Schiller, J., Adamescu, M., Ambrosio, R., Attermeyer, K., Bachi, G., Bègue, N., Bučas, M., Cabrera-Brufau, M., Camacho-Santamans, A., Carballeira, R., Carloni, M., Cavalcante, L., Cazacu, C., Checcucci, G., Coelho, P., Dinu, V., ... Camacho, A. (n.d.). Hydrological and landscape controls on dissolved organic matter dynamics in European wetlands: Implications for management and restoration. *Submitted to Biogeosciences*.
- Silva, J. P., Lasso, A., Lubberding, H. J., Peña, M. R., & Gijzen, H. J. (2015). Biases in greenhouse gases static chambers measurements in stabilization ponds: Comparison of flux estimation using linear and non-linear models. *Atmospheric Environment*, 109, 130–138. <https://doi.org/10.1016/J.ATMOSENV.2015.02.068>
- Stakėnienė, R., Jokšas, K., Kriauciūnienė, J., Jakimavičius, D., & Raudonytė-Svirbutavičienė, E. (2023). Nutrient Loadings and Exchange between the Curonian Lagoon and the Baltic Sea: Changes over the Past Two Decades (2001–2020). *Water* 2023, Vol. 15, Page 4096, 15(23), 4096. <https://doi.org/10.3390/W15234096>